



Micro- and nanogels with labile crosslinks – from synthesis to biomedical applications

Journal:	<i>Chemical Society Reviews</i>
Manuscript ID:	CS-REV-10-2014-000341.R1
Article Type:	Review Article
Date Submitted by the Author:	08-Dec-2014
Complete List of Authors:	Zhang, Xuejiao; Institut für Chemie und Biochemie, Malhotra, Shashwat; Institut für Chemie und Biochemie, Molina, Maria; Institut für Chemie und Biochemie, Haag, Rainer; Freie Universität Berlin, Institut für Chemie

**Micro- and nanogels with labile crosslinks — from synthesis to
biomedical applications**

Xuejiao Zhang, Shashwat Malhotra, Maria Molina, Rainer Haag*

*Institute of Chemistry and Biochemistry, Freie Universität Berlin, Takustrasse 3,
Berlin 14195, Germany*

Corresponding author:

Prof. R. Haag

Institute for Chemistry and Biochemistry

Freie Universität Berlin

Takustrasse 3, Berlin 14195 (Germany)

E-mail: haag@chemie.fu-berlin.de

Abstract

Micro- or nanosized three-dimensional crosslinked polymeric networks have been designed and described for various biomedical applications, including living cell encapsulation, tissue engineering, and stimuli responsive controlled delivery of bioactive molecules. For most of these applications, it is necessary to disintegrate the artificial scaffold into nontoxic residues with smaller dimensions to ensure renal clearance for better biocompatibility of the functional materials. This can be achieved by introducing stimuli-cleavable linkages into the scaffold structures. pH, enzyme, and redox potential are the most frequently-used biological stimuli. Moreover, some external stimuli, for example light and additives, are also used to trigger the disintegration of the carriers or their assembly. In this review, we highlight the recent progress in various chemical and physical methods for synthesizing and crosslinking micro- and nanogels, as well as their development for incorporation of cleavable linkages into the network of micro- and nanogels.

Keywords: Microgel, nanogel, covalent crosslinking, supramolecular crosslinking, labile linkage

List of abbreviation

ATRP	atom transfer radical polymerization
NMP	nitroxide-mediated polymerization
RAFT	reversible addition-fragmentation transfer
OEOMA	poly(oligo(ethylene oxide) monomethyl ether methacrylate)
DMA	dimethacrylate
GSH	glutathione
DOX	doxorubicin
PEO	poly(ethylene oxide)
GFP	Green fluorescent protein
PDMS	polydimethylsiloxane
DMAEMA	N,N'-dimethylaminoethyl methacrylate
dPG	dendritic polyglycerol
SPAAC	strain-promoted azide-alkyne cycloaddition
PEG-DIC	poly(ethylene glycol)-dicyclooctyne
hPEA-AGE	hyperbranched poly(ether amine)
PTMP	pentaerythritol tetra(3-mercaptopropionate)
TETA	triethylenetetramine
TEPA	tetraethylenepentamine
BAC	N,N'-bis(acryloyl)cystamine
TEOS	tetraethyl orthosilicate
DTT	dithiothreitol
Pox(mDOPA)	poly(methacrylamide)-bearing quinone

PAH	poly(allylamine)
TCEP	tris(2-carboxyethyl)phosphine
cRGD	cyclic arginine-glycine-aspartic acid
PDS	pyridyl disulfide
PEO-b-P(MEOMA-co-CMA)	poly[2-(2-methoxyethoxy)ethylmethacrylate -co-4-methyl-[7-(methacryloyl)oxyethoxy] coumarin]
PEEP	poly(ethyl ethylene phosphate)
PFp	pentafluorophenyl
PEG-PAsp	PEG-poly(aspartic acid)
PSI	poly(succinimide)
HMD	hexamethylenediamine
PEGdiacid	polyethylene glycol dicarboxylic acid
PMBV	poly(2-methacryloyloxyethyl phosphorylcholine - <i>co-n</i> -butyl methacrylate- <i>co</i> -4-vinylphenyl boronic acid)
PVA	poly(vinyl alcohol)
NIPAAm	N-isopropylacrylamide
MAAm-BO	5-methacrylamido-1,2-benzoxaborole
FPBA	2-formylphenylboronic acid
HRP	horseradish peroxidase
HPA	3-(4-hydroxyphenyl) propionic acid
GOD	glucose oxidase
APS	ammonium persulfate
HA	hyaluronic acid
rhGH	recombinant human growth hormone
PBAE	poly(β -amino ester)
ICG	indocyanine green
CHP	cholesterol-bearing pullulan
IL-12	Interleukin-12
BMP2	recombinant human bone morphogenetic protein 2
FGF18	recombinant human fibroblast growth factor 18
SLN	sentinel lymph node
DOCA-GC	deoxycholic acid-modified glycol chitosan
Ex4-C16	palmityl acylated exendin-4
TF	transferring protein
QDs	quantum dots
PNVF	poly(N-vinylformamide)
dex-HEMA	dextran hydroxyethyl methacrylate
DMAEMA	dimethyl aminoethyl methacrylate
GC	glycol chitosan
OEG	oligoethyleneglycol
PEG-P(HEMA-co-AC)	poly(ethylene glycol)-b-poly(2-(hydroxyethyl)

	methacrylate-co-acryloyl carbonate)	
CC	cytochrome C	
OEGA	oligo(ethylene glycol) acrylate	
DMDEA	2-(5,5-dimethyl-1,3-dioxan-2-yloxy)	ethyl acrylate
PTX	paclitaxel	
BADS	bis(2-acryloyloxyethyl) disulfide	
MRSA	methicillin-resistant strain of <i>staphylococcus aureus</i>	
ATP	Adenosine-5'-triphosphate	
Azo	azobenzene	
β -CD	β -cyclodextrin	
BSA	bovine serum albumin	

1. Introduction

Micro- and nanogels are crosslinked hydrogel particles with three-dimensional networks composed of water soluble/swellable polymers.^{1,2} This composition entails elastic moduli in the range of 0.1-100 kPa, which makes them a primary soft matter.³ Like hydrogels, their features are: high water content, biocompatibility, and desirable chemical and mechanical properties.⁴ In addition, their tunable size from nanometers (nanogels) to micrometers (microgels),^{3, 5} large surface area for multivalent bioconjugation, and interior network for the incorporation of biomolecules make them more advantageous than micelles, vesicles, liposomes, polymer prodrugs, etc. for biomedical applications.¹ Apart from drug delivery applications, micro- and nanogels have also great potential in the areas of bioimaging,⁶⁻¹² sensing,^{10, 13-20} antifouling,^{21, 22} DNA or siRNA delivery,²³⁻³⁰ and tissue engineering,³¹⁻³³ etc.

A stable blood stream in the delivery system is highly desirable for in vivo applications during systemic administration. Crosslinked networks, especially covalently crosslinked micro- and nanogels can prevent leakage of the payload, which enhances the therapeutic efficiency of the given drug. Upon reaching the target sites, the drug payload should be effectively released from the cargo. Therefore, the carriers are required to be able to respond to the relevant stimuli of the targeted disease, which is especially important for the burst release systems. Moreover, cytotoxicity is a crucial criterion in designing delivery vehicles. The degradable carrier systems not only can facilitate drug release under certain stimuli, but can also decrease the inherent toxicity by avoiding accumulation of the carrier vehicle via clearance from the body, after they complete their delivery tasks.

Cleavable linkages and degradable polymer backbones or pendant groups are often used to form degradable gel networks. Introducing reversible crosslinking groups onto precursor molecules that form labile crosslinkages via gelation, however, is most commonly applied to fabricate degradable micro- and nanogels.

Delivery of bioactive molecules is one of the most relevant fields for the applications

of micro- and nanogels. Various environmental stimuli, including internal (e.g. pH, redox potential, and enzyme) and external (light and additives), have been used to trigger the dissociation of micro- and nanogels, facilitating the drug release. Disulfide bonds are of great interest for making micro- and nanogels, since it is prone to rapid cleavage because of the high redox potential inside the cells.³⁴⁻³⁸ Another important intracellular signal, acidic pH, can trigger the degradation of micro- and nanogels with acid-cleavable linkages into the corresponding precursors or small molecules.^{29, 39-41} In addition, enzymes, existing with concentration specialty in different cells and tissues, are also used as an intracellular signal to induce site-specific drug release.^{42, 43}

With a focus on the cleavable linkages utilized in the crosslinked network of micro- and nanogels, this review goes beyond previous overviews. The first half section of this review spotlights the recent progress of synthetic strategies to produce covalently and supramolecular crosslinked micro- and nanogels. In the second half, cleavable linkages which are used in designing degradable micro- and nanogels have been highlighted. We emphasize the importance of degradable linkers which are incorporated in the network of biodegradable micro- and nanogels and subsequently affecting their biomedical efficacies as well as their fate.

2. Strategies to produce micro- and nanogels

A wide variety of methodologies have been developed to prepare micro- and nanogels. In the current review, we focus on inverse miniemulsion, microfluidics, and inverse nanoprecipitation which are important techniques used during the synthesis of micro- and nanogels. In brief, inverse miniemulsion is a water-in-oil (W/O) heterogeneous polymerization process, which contains template nanodroplets formed by oil-soluble surfactants in a continuous organic medium.⁴⁴ In the microfluidic method, glass capillary devices or devices made by the soft lithography, normally composed of polydimethylsiloxane (PDMS) can be used for droplet fabrication.⁴ The nanoprecipitation technique is novel for preparing hydrophilic nanogels.⁴⁵ Size defined nanogel particles are generated during in situ crosslinking of the precursors in the surfactant free water droplet.

Currently, covalent crosslinking (including polymerization of low molecular weight monomers as well as crosslinking of macromolecular precursors), and supramolecular crosslinking approaches can be used for the preparation of micro- and nanogels. Covalently crosslinked micro- and nanogels are formed by coupling reactive functional groups, which allow making the structure and properties of the gel particles tunable. By introducing labile bonds into the networks during covalent crosslinking, a variety of degradable micro- and nanogels were synthesized for drug delivery applications. Supramolecular crosslinked micro- and nanogels are based on the self-assembly of polymers through noncovalent interactions. The details of these strategies are discussed in the subsequent sections.

2.1. Covalent crosslinking

Covalent crosslinking methodologies are the basis for covalent coupling of the reactive functional groups in the low molecular weight monomers or macromolecular precursors to form the gel networks. Micro- and nanogels formed by covalent bonds via chemical crosslinking possess colloidal stability under *in vivo* conditions, which is essential for leakage of drug release induced by unwanted dissociation of the gel network. Covalent crosslinking strategies mainly include radical polymerizations, click chemistries, Schiff-base reaction, thiol-disulfide exchange reaction, and photoreactions (see Table 1).

2.1.1. Radical polymerization

Radical polymerization, especially living radical polymerization such as atom transfer radical polymerization (ATRP), nitroxide-mediated polymerization (NMP), and reversible addition-fragmentation transfer (RAFT), have been used to synthesize micro- and nanogels.^{46, 47} Free radicals, normally generated from the initiator molecules, are used to initiate the polymerization, and monovinyllic monomers are crosslinked with di- or multifunctional crosslinkers to form the micro- and nanogel networks within preformed colloidally self-assembled droplets.⁴⁶ Some important examples in this category are listed in the following.

Matyjaszewski et al. have synthesized stable biodegradable nanogels by an ATRP of poly(oligo(ethylene oxide) monomethyl ether methacrylate) (OEOMA) in inverse miniemulsion in the presence of a disulfide-functionalized dimethacrylate (DMA) crosslinker (Figure 1).⁴⁸ These nanogels are biodegradable in the presence of the tripeptide, glutathione, which not only can trigger the release of the encapsulated payload, including rhodamine 6G and doxorubicin (DOX), but also facilitates the clearance of blank carriers. Furthermore, the OH-functionalized nanogels can be easily decorated with biotin via an esterification reaction.

Figure 1. (a) Chemical structures of the crosslinker DMA and glutathione ethyl ester. (b) Synthesis of biodegradable nanogels by ATRP and functionalization of nanogels with biotin. Reprinted with permission from ref. 48. Copyright 2007 American Chemical Society.

Matyjaszewski and coworkers have further synthesized biocompatible and uniformly crosslinked nanogels based on poly(ethylene oxide) by inverse miniemulsion ATRP. This nanogel system was capable of encapsulating and delivering a variety of payloads, including inorganic, organic, and biological molecules. The endocytotic properties of these nanogels make them good candidates for various drug delivery applications.⁴⁹ They also used a genetically engineered protein, which contained a nonnatural amino acid with an ATRP initiator, to fabricate protein-nanogel hybrids by electron transfer (AGET) ATRP in inverse miniemulsion.⁵⁰ The green fluorescent protein (GFP), which was covalently conjugated into the nanogels, preserved its native tertiary structure, thus demonstrating its potential use for controlled release applications.

Compared to nanogels prepared by the conventional radical polymerization, nanogels synthesized via ATRP have more advantages, such as higher swelling ratios, better colloidal stability, more homogenous and controlled structures, and controlled degradation.^{44, 50} However, remaining copper salts can be problematic for in vivo applications.

In addition to ATRP, RAFT polymerization has also been used for the fabrication of nanogels. Yan et al. have reported the synthesis of cationic nanogels by a one-step surfactant-free RAFT process. An amphiphilic PEGylated macroRAFT agent (mPEG₅₅₀-TTC) was used to form and stabilize the micelle, where the polymerization and crosslinking of N,N'-dimethylaminoethyl methacrylate (DMAEMA) monomer were performed.⁵¹ Thermoresponsive, acid degradable core-crosslinked nanogels were synthesized by the group of Narain via RAFT polymerization technique. These nanogels can be efficiently degraded and release the encapsulated protein below pH 6.⁵²

2.1.2. Click chemistry

2.1.2.1. Copper-catalyzed azide-alkyne Huisgen cycloaddition (CuAAC)

The CuAAC reaction is a modular approach to couple two reactive components in a fast, versatile, regioselective, and highly efficient reaction.⁵³ Normally, click reactions are performed under mild conditions without the formation of byproducts (atom conservation). Furthermore, both azides and alkynes are inert towards biological molecules,⁵⁴ which is propitious for the synthesis of biomaterials. Our group recently reported the synthesis of hydrophilic polyglycerol based nanogels crosslinked through a facile click reaction by miniemulsion.^{55, 56} Dendritic polyglycerol (dPG) was modified with alkynes or azides to form the complementary reactants, that were miniemulsified in equimolar, which after catalysis of copper salts, resulted in crosslinked particles. Later on, a mild, surfactant free inverse nanoprecipitation method was developed in our group, through which polyglycerol nanogels were obtained with the defined size from 100 nm to 1000 nm by bioorthogonal copper catalyzed click chemistry (Figure 2a). Biodegradability was achieved by the introduction of benzacetal bonds into the nanogel network. Labile enzymes were well-protected by these nanogels in the process of encapsulation and retained their activity and structural integrity after being released.⁴⁵

Figure 2. (a) Reverse nanoprecipitation process for nanogel formation. Injection of an aqueous solution of azide functionalized polyglycerol (red spheres), alkyne functionalized polyglycerol (blue spheres), and a 3D protein structure. Formation of a particle template after the aqueous phase diffused into the acetone phase. Crosslinking by CuAAC is achieved due to upconcentration. (b) Degradation of polyglycerol nanogels at different pH determined by UV/vis absorption. (c) Release kinetics of protein from nanogel network at different pH determined by HPLC. Reproduced from ref. 45. Copyright 2013 Elsevier Ltd.

Similarly, Anderson et al. have generated dextran based nanogels with controllable surface functionalities and targeting properties by a facile approach via click chemistry in an inverse emulsion.⁵⁷ Cu^{+2} and sodium ascorbate were used to initiate the click reaction between alkyne- and azide-dextran in the aqueous phase before emulsification. The free alkyne/azide groups after click chemistry allowed surface modification of nanogels, for example, by azido-containing bisphosphonate and alkyne-containing Alexa Fluor 647. The nanogels were degradable in the presence of enzyme dextranase and showed modular distribution and targeting properties for bone disease. However, the incomplete removal of copper catalysts is problematic for in vivo applications. Therefore, copper-free click methods can be advantageous.

2.1.2.2. Copper-free click chemistry

Most recently, copper-free click reactions, including strain-promoted azide-alkyne cycloaddition (SPAAC), thiol-ene click reaction, and Michael addition reaction, make it possible to synthesize micro- and nanogels without any potentially toxic catalysts that are commonly required,⁵⁸ thus beneficial for the biomedical applications.

2.1.2.2.1. Strain-promoted azide-alkyne cycloaddition (SPAAC)

CuAAC is not suitable for encapsulating labile biomolecules since copper can be cytotoxic for living cells.⁵⁹ The noncytotoxic and efficient SPAAC have been developed as an alternative to CuAAC for synthesizing hydrogels for biomedical applications, especially in the field of tissue engineering.^{41, 60} Recently, our group has developed pH-cleavable cell-laden microgel systems by combining bioorthogonal SPAAC and droplet-based microfluidics for the encapsulation and programmed release of cells (Figure 3a,b,c).³² Homo-bifunctional poly(ethylene glycol)-dicyclooctyne (PEG-DIC) and dPG-polyazide were prepared and used as macromonomers for in situ crosslinking to obtain microgels by SPAAC. The viability of the encapsulated cells can be retained for a long time when cultured inside the microgels.

Figure 3. Cell encapsulation and release: (a) Preparation of dPG-azide precursors and injection of precursors and cells into a microfluidic device. (b) Formation of cell-laden microgels with high viability determined by fluorescent live-dead assays. (c) Degradation of microgels. Degradation of microgel particles (d) at different pH values and fluorescence images of one microgel particle incubated at pH 4.5 (e) at the beginning, (f) half-completed degradation, and (g) fully-completed degradation. Reprinted with permission from ref. 32. Copyright 2013 WILEY-VCH.

2.1.2.2.2. Thiol-ene click reaction

In addition to SPAAC, thiol-ene reaction is another click reaction that does not need a metal catalyst. Typically, thiols are reacted with unsaturated groups, e.g. alkenes, in a

thiol-ene reaction. The research group of Jiang has fabricated a multi-responsive microgel based on thiol-ene photo-click crosslinking after the co-assembly of the amphiphilic allyl glycidyl ether ended hyperbranched poly(ether amine) (hPEA-AGE) and pentaerythritol tetra(3-mercaptopropionate) (PTMP).⁶¹ After self-assembly, the inner core which is composed of hydrophobic PPO chains and PTMP was crosslinked upon irradiation by UV light.

2.1.2.2.3. Michael addition

Typically, the Michael addition reaction is the base-catalyzed nucleophilic addition of Michael donor (i.e. enolate anion) to an activated α,β -unsaturated carbonyl-containing compound, a so-called Michael acceptor.⁶² Michael addition has also been used to make micro- and nanogels without any metal additive.

Seiffert et al. developed monodispersed cell-laden microgels via the nucleophilic Michael addition of dithiolated PEG with acrylated hyperbranched polyglycerol (hPG) through droplet microfluidic templating (Figure 4).⁶³ After the formation of premicrogel by injecting of both precursor solutions together with a cell-containing solution into a microfluidic device, the gelation proceeds to produce cell-laden microgels.

Figure 4. Formation of microgels by crosslinking hPG and PEG via Michael addition. Reprinted with permission from ref. 63. Copyright 2012 American Chemical Society.

The research group of Zhang has developed degradable nanogels with cleavable disulfide bonds and amine groups in a network that has been crosslinked by the Michael addition of triethylenetetramine (TETA) or tetraethylenepentamine (TEPA) with *N,N'*-bis(acryloyl)cystamine (BAC).⁶⁴ As shown in Figure 5, mesoporous silica spheres were obtained after hydrolyzing tetraethyl orthosilicate (TEOS) that has been catalyzed by the amine groups inside the nanogel network and after removing the nanogel scaffold by cleaving the disulfide bonds.

Figure 5. The formation of mesoporous silica spheres from hybrid silica colloids by removal of the nanogels with DTT. Reprinted with permission from ref. 64. Copyright 2009 American Chemical Society.

2.1.3. Schiff-base reaction

The Schiff-base reaction occurs between aldehydes and amines or hydrazide containing compounds. It has been used to generate biocompatible gels due to its mild reaction conditions.

Qu and Yang et al. have generated protein nanogels crosslinked by a one-step Schiff-base reaction between the amino groups of urokinase and benzaldehyde bifunctionalized PEG.⁶⁵ The formation of imine bonds, which are stable under physiological conditions and labile at acidic pH, makes these nanogels promising

candidates for the intracellular delivery of proteins.

Detrembleur et al. have described a novel approach to fabricate antibacterial, antibiofilm, and antiadhesion platforms based on functional nanogels, which were crosslinked through the Schiff-based reaction and/or Michael addition reaction between poly(methacrylamide)-bearing quinone (Pox(mDOPA)) and poly(allylamine) (PAH).⁶⁶ In order to introduce the antibacterial properties, silver was loaded into the nanogels, which was beneficial for the Michael addition but prevented the Schiff-base formation due to the complexation of quinone groups with silver.

2.1.4. Thiol-disulfide exchange reaction

In thiol-disulfide exchange reaction, the deprotonated free thiol displaces one sulfur of the disulfide bond in the oxidized species.⁶⁷ This is essential for cellular disulfide bond formation and is now commonly used in formation of nanogels. Zhong et al. prepared reversibly crosslinked dextran nanoparticles from dextran-thioctic acid derivatives based on thiol-disulfide exchange reaction using a catalytic amount of dithiothreitol (DTT).⁶⁸ Thioctic acid is naturally produced in the human body⁶⁹ and showing no cytotoxicity even at high concentration.⁷⁰ Recently, our group reported the preparation of a dual-responsive prodrug nanogel for the covalent conjugation and intracellular delivery of doxorubicin (DOX) through a thiol-disulfide exchange reaction by an inverse nanoprecipitation method.³⁸ As shown in Figure 6, the macromolecular precursor was synthesized by the conjugation of thioctic acid with hPG. A predetermined amount of DTT was used to initiate the thiol-disulfide exchange reaction by cleaving the lipoyl ring in thioctic acid to the corresponding dihydrolipoyl groups. The nanogel with disulfide crosslinked network can be degraded under intracellular reductive conditions into small fragments, which are below the clearance limitation of the kidneys (~ 50 kDa). DOX was conjugated with an acidic labile hydrazone linker to form the prodrug nanogel, which can efficiently deliver and release the drug payload into the nucleus.

Figure 6. Synthetic approaches of nanogel and prodrug nanogel. Reprinted with permission from ref. 38. Copyright 2014 Elsevier Ltd.

Xu et al. have designed a nano cocktail of a nanogel system by thiol-disulfide exchange reaction that was initiated by adding a deficient amount of tris(2-carboxyethyl)phosphine (TCEP).³⁷ This nanogel is sensitive to both acidic pH and redox potential. Drug loaded nanogels, ND (nano DOX) and NCPD (a nano cocktail of paclitaxel and DOX), are stable under physiological conditions and yet spontaneously swell and quickly release their payload after entering the cancer cells with the help of a targeting peptide, cRGD. A synergistic anticancer effect is accomplished in the case of NCPD owing to its elevated internalization and dual responsiveness property.

The research group of Thayumanava has fabricated a series of nanogel systems based on the thiol-disulfide exchange reaction, which causes a self-crosslinking of pyridyl disulfide (PDS) containing amphiphilic polymers.^{35, 36, 71-73} The addition of deficient

amounts of DTT reduces the controlled amount of PDS groups to thiols, which further exchange with the remaining PDS groups affording a crosslinked nanogel. In the process of thiol-disulfide exchange, the byproduct, pyridothione, formed. The crosslinking density can be calculated by detecting the concentration of pyridothione through UV-vis. By introducing tri-arginine, which provides both the positive charge and cell-penetrating property, to the surface of the charge-neutral nanogel, they successfully combined the encapsulation of lipophilic small molecules and binding proteins in one single nanogel system.⁷³

Wu et al. have described an approach to fabricate controllable micro- and nanogels via a pH-responsive thiol-disulfide exchange reaction of the disulfide-linked core-shell hyperbranched polymer through an inverse emulsion technique.⁴³ In the process of basification-triggered disulfide reshuffling, the shells dissociated and the cores were crosslinking. By varying the gelation time, loose and compact micro- and nanogels with distinct particle sizes and swelling capacities were obtained.

2.1.5. Photo-induced crosslinking

Reactants containing a photo-activatable group can be crosslinked by photo irradiation. Zhao and coworkers have prepared photoresponsive nanogels via photo-crosslinking based on the reversible photodimerization and photocleavage of coumarin.^{74, 75} A block of Poly(ethylene oxide) and a block of poly[2-(2-methoxyethoxy)ethylmethacrylate-co-4-methyl-[7-(methacryloyl)oxyethoxy]coumarin] (PEO-b-P(MEOMA-co-CMA)) formed micellar aggregates when the temperature was above its lower critical solution temperature (LCST), and the dimerization of coumarin side groups was initiated upon UV irradiation at $\lambda > 310$ nm via photo-crosslinking, generating the water-soluble nanogels upon cooling to $T < LCST$.

Wang et al. have synthesized biodegradable nanogels by the photo-crosslinking of salt-induced poly(ethyl ethylene phosphate) (PEEP) assemblies with a template-free method.⁷⁶ Upon addition of salt, PEEP self-assembled into core-shell nanoparticles due to its hydrophobic-to-hydrophilic transition property induced by salt. The crosslinked hydrophilic nanogels were obtained after UV-irradiation and removal of the salt by dialysis. Although photo-induced crosslinking is highly efficient, the initiator may induce cytotoxicity in the produced gels.⁷⁷ Therefore, it is important to choose the photoinitiator to make biocompatible gel networks.

2.1.6. Amide-based crosslinking

Due to the high reactivity with carboxylic acids, activated esters, isocyanates, etc., amine groups can be used for synthesizing micro- and nanogels.⁷⁸ This facile methodology provides the opportunity to introduce various stimuli-response properties into the nanogels by modulating the structure of the diamine crosslinker.

Thayumanavan et al. have developed a facile approach to synthesize hydrophilic nanogels based on a simple reaction between pentafluorophenyl (PFP)-activated hydrophobic esters and diamine crosslinkers.⁷⁹ As shown in Figure 7, PFP moieties

not only serve as the crosslinking reagents, but are also used for further functionalizing the nanogels and providing lipophilic domains inside the nanogel for encapsulation of the hydrophobic drugs.

Figure 7. Schematic illustration of synthesis and surface modifications of the crosslinked nanogels. Reprinted with permission from ref. 79. Copyright 2012 American Chemical Society.

Kim et al. fabricated pH-responsive PEG-poly(aspartic acid) (PEG-PAsp) nanogels by crosslinking the amine-reactive hydrophobic poly(succinimide) (PSI) with the crosslinker hexamethylenediamine (HMD) through a nucleophilic ring-opening reaction, followed by hydrolyzing hydrophobic core (Figure 8).⁸⁰ The crosslinking degree was adjusted by varying the crosslinker feed ratio, and the nanogel swelled in water up to 30 times of its original volume. In acidic conditions, the deswelling of the nanogels retarded the release of the protein payload.

Figure 8. Synthesis of the PEG-PAsp nanogel. Adapted from ref. 80. Copyright 2013 Royal Society of Chemistry.

Iturbe et al. have generated chitosan based nanogels by reacting the amine of chitosan with dicarboxylic acid-decorated chitosan in water-in-oil (W/O) microemulsion.⁸¹ Two biocompatible dicarboxylic acids, polyethylene glycol dicarboxylic acid (PEGdiacid) and tartaric acid, were used, whereby the PEGdiacid was more efficient than the tartaric acid when crosslinking with chitosan.

2.1.7. Boronic acid-diol complexation

The complexation between boronic acid and 1,2- or 1,3-diols has been applied to fabricate hydrogels^{34, 82-87} and core-crosslinked micelles^{88, 89}. Recently, boronate esters have also been utilized to prepare nanogels. Ishihara et al. have prepared spherical polymeric hydrogels via specific esterification between phenyl boronic acid groups in poly(2-methacryloyloxyethyl phosphorylcholine-*co-n*-butyl methacrylate-*co*-4-vinylphenyl boronic acid) (PMBV) and hydroxyl groups in poly(vinyl alcohol) (PVA) by a flow-focusing microfluidic channel device.⁹⁰ The polymer distribution in the gel was influenced by the PVA concentration, which was expected to facilitate fine-tuning of the mechanical and permeation properties of the hydrogel particles. Individual cells could be encapsulated and remained viable in the hydrogel particles.

Narain et al. have made use of the boronic–diol complexation to synthesize responsive hydrogels and nanogels by simply mixing the well-defined glycopolymer and P(NIPAAm-*st*-MAAmBO)s copolymers, which were statistically copolymerized from N-isopropylacrylamide (NIPAAm) and 5-methacrylamido-1,2-benzoxaborole (MAAm-BO) (Figure 9a).⁹¹ As shown in Figure 9b, by adding a superfluous glucose, the glycopolymer dissociated from the P(NIPAA₉₀-*st*-MAAmBO₁₂), which instantly associated with the added free glucose molecules. When the clear solution was

dialyzed against an alkaline solution, spherical nanogels could be obtained. As the small glucose molecules passed through the dialysis membrane, the P(NIPAA₉₀-*st*-MAAmBO₁₂) chain could again gradually interact with glycopolymer chains.

Figure 9. (a) Formation of gel by boronic-diol interaction between P(NIPAAm-*st*-MAAmBO) and glycopolymers. (b) Formation of nanogels by adding excess free glucose solution into the gel sample and extensive dialysis in pH 12 solution at 4 °C, and a TEM image of the nanogels. Reprinted with permission from ref. 91. Copyright 2013 American Chemical Society.

Our group has recently developed a novel ATP- and pH-responsive degradable nanogel system based on the complexation of 1,2-diols in dPG, and boronic acids, which are conjugated with dPG as the macromolecular crosslinker (Figure 10). dPG was converted into 100% functionalized dPG-amine (dPGA), and then 2-[2-(2-methoxyethoxy) ethoxy] acetic acid was conjugated with amine groups by amide coupling with the purpose of eliminating the cytotoxic effect induced by amines. The macromolecular crosslinker, dPG-Am-PEG-FPBA, was synthesized via a Schiff-base reaction between the amino groups in dPGA and formyl groups in 2-formylphenylboronic acid (FPBA), followed by the reduction with NaBH₄. The dual-responsive nanogel, composed of dPG as the scaffold and dPG-Am-PEG-FPBA as the macromolecular crosslinker, was fabricated via the surfactant-free inverse nanoprecipitation method.^{45, 92}

Figure 10. Synthetic approaches of boronic ester nanogels and Methotrexate (MTX)-loaded nanogels. Reprinted with permission from ref. 92. Copyright 2014 WILEY-VCH.

2.1.8. Enzyme-catalyzed crosslinking

Enzyme-catalyzed crosslinking has been used for the preparation of hydrogels as an innovative technology with greater efficiency than other crosslinking methods due to its short reaction time, mild reaction condition, and high biocompatibility.⁹³⁻⁹⁵ The gelation kinetics, depending on the structure and composition of the macromer, the ratio of the reactants, and the enzyme concentration, are well-controllable. Therefore, enzyme-catalyzed reaction is suitable for in situ gelation systems. So far, however, the enzyme-catalyzed nanogels have not been widely investigated.

Groll and coworkers have presented redox-sensitive disulfide-crosslinked hydrogels and nanogels by horseradish peroxidase (HRP)-mediated crosslinking without using hydrogen peroxide (H₂O₂).⁹⁶ The cytocompatible hydrogels served as cell-laden without destroying their vitality. By adding thiol-decorated peptides during the nanogel's formation, peptide-functionalized nanogels can be obtained. β -galactosidase was loaded as a model protein into the HRP crosslinked nanogel and could be released after degrading the nanogels under the cytosol's reductive conditions.

Recently, our group developed biocompatible hydrogels based on HRP catalyzed

crosslinking of 3-(4-hydroxyphenyl) propionic acid functionalized hyperbranched polyglycerol (hPG-HPA) in the presence of H_2O_2 for living cells encapsulation (Figure 11).⁹⁷ The formation of hydrogel can be triggered by glucose in the presence of GOD and HRP since the oxidation of glucose by glucose oxidase (GOD) can produce H_2O_2 .

Figure 11. Illustration of hPG-HPA hydrogel formation by HRP crosslinking. Reprinted with permission from ref. 97. Copyright 2014 American Chemical Society.

2.1.9. Siloxane crosslinking

Jandt et al. have fabricated temperature-sensitive poly(N-isopropylacrylamide) microgels based on the hydrolysis/condensation of siloxane groups by free radical precipitation.^{98, 99} The thermal initiator, ammonium persulfate (APS), was used to initiate the radical copolymerization of NIPAAm, as well as to catalyze the hydrolysis/condensation of siloxane groups due to the acidic environment caused by APS. This method has not yet been used for biomedical gel synthesis.

In summary, the formation of micro- and nanogels by covalent crosslinking approaches can maintain their stability in a complex and harsh environment (e.g. in vivo conditions), prevent the leakage of the encapsulated drug payload, and enhance their therapeutic efficacy. However, traditional covalent crosslinking normally involves crosslinking agents, which sometimes cause unwanted toxic effects and damage the entrapped fragile substances, including proteins or cells. Therefore, more and more biocompatible and bioorthogonal reactions are continuously emerging in the field of biomedical gelation which also needs further exploration.

2.2. Supramolecular crosslinking

Micro- and nanogels formed by supramolecular crosslinking involve self-assembled aggregations based on various physical interactions including ionic, hydrophobic, and hydrogen bonding. Unlike the covalent crosslinking method, supramolecular crosslinking which does not need any crosslinking agent that might cause unwanted interaction with the bioactive substances during the encapsulation of biomacromolecules. Moreover, the preparative conditions of supramolecularly crosslinked gels are normally mild, mostly in water, which avoids the adverse toxic effects. However, gels formed by the supramolecular crosslinking may possess less mechanical strength and stability to face the harsh in vivo conditions present in blood circulation which makes them less applicable than covalently crosslinked gels.¹⁰⁰

2.2.1. Ionic interaction

The research group of Ryu developed a versatile method for synthesizing self-assembled supramolecular nanogel by electrostatic interaction between positively

charged surfactant micelles and negative polypeptides.¹⁰¹ Below the critical micelle concentration (CMC) of the small positive surfactants, supramolecular ionic amphiphilicities were formed due to the interaction between individual positive surfactants and negatively charged gelatin B. Further self-assembly of the supramolecular amphiphilicities induced larger nanoaggregates that were driven by the hydrophilic-hydrophobic balance. Above the CMC, the small positive surfactants first self-assembled into positively charged micelles and then interacted with gelatin B with negative charge which resulted in core-shell-like aggregates. These core-shell-like nanogel aggregates contained stable hydrophobic pockets that prevented the hydrophobic guests from diffusing, thereby increasing the encapsulation stability.

Nakai and Akiyoshi et al. have developed anionic nanogels based on the self-assembly of cholesteryl-group-bearing hyaluronic acid (HA) for protein delivery.¹⁰² Compared to the conventional non-ionic nanogels, the anionic HA nanogels can efficiently bind a variety of proteins without denaturation. An injectable hydrogel was formed by the association of HA nanogel induced by salt, showed a sustainable release of recombinant human growth hormone (rhGH) in rats for one week.

Lim et al. fabricated nanogels with pH-sensitivity and targeting ability that were composed of CD44-receptor-targeting hyaluronic acid (HA), pH-sensitive poly(β -amino ester) (PBAE), and near-infrared (NIR) fluorescent indocyanine green (ICG) that can be incorporated into the assembled structure of HA and PBAE polymers based on the electrostatic and hydrophobic interactions.⁹ On decreasing the pH from 7.4 to 5.5, the nanogel disassembled due to the protonated PBAE so that the fluorescence intensity increased which resulted in the liberation of the probes from the nanogels.

2.2.2. Hydrophobic interaction

Cholesterol is frequently used as a hydrophobic moiety to induce the self-assembly of amphiphilic copolymers to form a nanogel structure based on the hydrophilic/hydrophobic balance.^{7, 8, 31, 103-107} Akiyoshi et al. fabricated hydrogel nanoparticles (nanogels) by the self-assembly of cholesterol-bearing pullulan (CHP).^{108, 109} CHP nanogels were physically entrapped into a three-dimensional hydrogel network, which was covalently crosslinked by HA modified 2-aminoethyl methacrylate via Michael addition. The embedded nanogel and hydrogel matrix synergetically achieved both loading and controlled release of protein without denaturation.¹⁰⁴ Akiyoshi et al. then made hybrid PEG hydrogels based on the crosslinking of CHP nanogels and nanogel-coated liposome complexes with pentaerythritol tetra(mercaptoethyl) polyoxyethylene by Michael addition. During the hydrolysis of the hydrogel under physiological conditions, the nanogel is released first and then the nanogel-coated liposomes. A variety of guest molecules can be loaded inside the nanogel/liposomes and also released in a controllable two-step profile in the hybrid hydrogels, which exhibit their capability for a multiple delivery of drugs, proteins, or DNA.¹⁰⁷ Moreover, they generated a raspberry-like assembly of nanogels

based on the Michael addition by crosslinking acrylate-modified cholesterol-bearing pullulan nanogel (CHPANG) with thiol-modified poly(ethylene glycol) (PEGSH) (Figure 12).¹⁰³ Interleukin-12 (IL-12) encapsulated with high efficiency (96%) in these nanogels can maintain a high level in mice plasma after subcutaneous injection. Later on, the same research group created fast-degradable hydrogels by crosslinking the aggregation of cholesteryl- and acryloyl-bearing pullulan (CHPOA) nanogels with PEGSH (Figure 12). Two distinct growth factors, recombinant human bone morphogenetic protein 2 (BMP2) and recombinant human fibroblast growth factor 18 (FGF18), were encapsulated in the nanogels, and CHPOA-FGF18+BMP2/hydrogel could more strongly enhance bone repair than the single protein-loaded hydrogel system.³¹

Figure 12. Structures of CHPOA, CHPANG, and PEGSH. Adapted from ref. 31 and 103. Copyright 2012 and 2009 Elsevier.

Lim et al. have reported the synthesis of a new near-infrared (NIR)-emitting polymer nanogel (NIR-PNG) using self-assembled pullulan-cholesterol nanogels conjugated with IRDye800.⁷ The resultant systems could be used for sentinel lymph node (SLN) mapping in both small and large animal models by optimizing the size for lymph node uptake.

Gref and coworkers presented a spontaneous formation of supramolecular nanoassemblies (nanogels) based on inclusion complexes between alkyl chain containing dextran and the molecular cavities containing β -cyclodextrin polymer.¹¹⁰ The uncomplexed cyclodextrin units were accessible for guest molecules, such as benzophenon or tamoxifen, representing the carrier potential of nanogels. They have further studied the stability of these supramolecular nanoassemblies (nanogels).¹¹¹ At low concentrations, the mean diameter of the nanogel suspensions did not vary much during storage. However, the concentrated ones tended to destabilize over time with increased mean diameter due to particle aggregation and/or fusion.

Youn et al. prepared inhalable nanogels by the self-assembly of deoxycholic acid-modified glycol chitosan (DOCA-GC) with palmityl acylated exendin-4 (Ex4-C16) based on hydrophobic and ionic interactions.¹¹² DOCA-GC nanogels showed tolerable cytotoxicity and did not induce any significant difference in the tissue histology of mouse lungs after pulmonary administration. The Ex4-C16-loaded DOCA-GC nanogels represented a sustained inhalation delivery system for treating type 2 diabetes. Normally, multiblock copolymers or graft copolymers, composed of a water-soluble polymer backbone, are capable of forming self-assembled aggregated gel particles.

Davis and coworkers presented the first in-human phase I clinical trial of targeted siRNA delivery system based on the inclusion complexes of cyclodextrin-decorated polymer (CDP) and adamantine terminated PEG (AD-PEG) (Figure 13).¹¹³ A human transferring protein (TF) targeting ligand was introduced on the exterior of the nanoparticles to attach TF receptors on the surface of the cancer cells. The targeted nanoparticles exhibited a dose-dependent accumulation in human tumors, which

induced a specific gene inhibition.

Figure 13. Formation of targeted nanoparticles. Reprinted with permission from ref. 113. Copyright 2010 Nature Publishing Group.

2.2.3. Hydrogen bonding

The supramolecular hydrogen bonding between the functional groups in the polymers, including $-OH$, $-NH_2$, etc., is an option for fabricating supramolecularly crosslinked gel networks. However, the network formed via hydrogen bonding lacks stability, since hydrogen bonding depends on the type of solvents and pH of the solution. The group of Park developed heparin nanogels based on nanocomplexes between thiolated heparin and PEG via hydrogen bonding, followed by the intermolecular crosslinking of disulfide bonds between thiolated heparin molecules by ultrasonication.¹¹⁴ These nanogels not only enhanced the internalization of heparin but also released them under the reductive cytosol environment, which resulted in the inhibition of cell proliferation and caspase-mediated apoptotic cell death.

Zhou et al. reported in-situ immobilization of CdSe quantum dots (QDs) into the chitosan-based hybrid nanogels formed either by noncovalent physical associations, such as secondary forces (hydrogen bonding or hydrophobic association) and physical entanglements, or by covalent crosslinkages.¹⁹ Unfortunately, these physically associated hybrid nanogels were unstable even under physiological pH, inducing significant cytotoxicity.

Feng et al. have constructed pH-sensitive nanohydrogels that were based on the supramolecular hydrogen-bonding of a cationic hyperbranched polycarbonate.¹¹⁵ The nanohydrogels expanded to a high degree in response to slightly decreased pH values from 7.4 to 6.6 due to the charge repulsion, which resulted in local release of the drug under acidic microenvironment.

Seiffert and coworkers prepared a series of poly(N-isopropylacrylamide) (pNIPAAm) with different types of crosslinkable sidegroups. By adding low molecular weight linkers that are complementary to the motifs on the polymer, different supramolecular polymer networks with greatly varying rheological properties were formed due to multiple hydrogen bonding.¹¹⁶ Then they fabricated linear polyglycerol-based multiresponsive supramolecular hydrogels crosslinked by hydrogen bonding, metal complexation, or both (Figure 14).¹¹⁷ Linear azide-functionalized polyglycerol is modified either with diaminotriazine and terpyridine or with cyanurate and terpyridine. Gelation occurs after mixing the aqueous solution of both compounds because of the multiple hydrogen bonding or the metal complexation in the presence of an iron (II) salt. Metal complexation-based crosslinking is used to develop hydrogels,¹¹⁸⁻¹²² but has not been applied for the fabrication of micro- and nanogels till now.

Figure 14. Supramolecular hydrogels formation crosslinked by multiple hydrogen bonding and metal complexation. Reprinted with permission from ref. 117. Copyright 2014 American Chemical Society.

It is not easy to prepare supramolecularly crosslinked micro- and nanogels with high stability and controlled size because the noncovalent bonds, including ionic interaction, hydrophobic interaction, and hydrogen bonding, are not strong enough. Nevertheless, their preparation process is relatively easy because it does not require toxic reagents or catalysts, and does not produce byproducts, which makes it favorable for biomedical applications. Furthermore, multivalent systems, containing multiple interactions, can further enhance their stability.¹²³

3. Cleavable covalent crosslinks

The stability of crosslinked micro- and nanogels is essential under certain circumstances, i.e. during blood circulation for drug delivery. However, permanent stability is not an option in some applications as the entrapped payload needs to be released at the target site for its biological functions. By introducing labile linkers into the scaffolds of the micro- and nanogels, reversible crosslinking can be realized at the target site. In this case, the stable structure of covalently crosslinked micro- and nanogels is broken down in response to certain stimuli. In the subsequent sections, we will focus on the cleavable crosslinks, including pH-cleavable, photo-cleavable, redox-cleavable, enzyme-cleavable, additive-cleavable crosslinks, etc. (see Table 2), which help to release the payload at the diseased site in a more efficient manner.

3.1. Acid-cleavable

The introduction of acid-cleavable crosslinks into the gel networks should favor the dissociation of gels, since the acidic conditions present in tumor tissues, endosomes (5.5-6.5), or lysosomes (4.5-5.5) can be responsible for the cleavage of acid-sensitive crosslinks. The pH value in normal tissues and blood is around 7.4, while in tumor or inflammatory tissues, the environment is 0.5-1.0 pH units lower. During cellular uptake, the vehicles first reach early endosome with a pH about 6, followed by late endosome, where the pH drops to 5-6. Subsequently, the vehicles can reach a more acidic compartment, the lysosome (pH ~ 4.5).¹²⁴⁻¹²⁶ These pH gradients existing in biological systems can be used as a trigger to fabricate acid sensitive gel systems for biomedical applications. Various acid-cleavable linkers have been applied into micro- and nanogel networks such as acetals or ketals, esters, imine, hydrazone, and vinyl ether. The incorporation of such linkers inside the micro- and nanogels will be examined in detail in the upcoming sections.

3.1.1. Acetal and ketal linker

3.1.1.1. Acetal linker

Bulmus and coworkers have prepared acid-labile microgel particles with divinyl-functionalized acetal-based crosslinkers via an inverse emulsion polymerization technique.¹²⁷ They have synthesized a number of

di(acrylate)-functionalized, acetal-based crosslinkers, and found that the *para*-substituent group on the benzene ring of the benzaldehyde acetal and the microenvironment polarity of the crosslinker structure can affect the hydrolysis rate. Crosslinkers, which were stable at neutral pH for a long time and underwent complete hydrolysis at slightly acidic pH in less than 1 h, were obtained. Rhodamine B-labeled dextran and BSA, as the model biomacromolecules, could be efficiently loaded into the microgels. The drug release could be controlled by adjusting the pH of the environment, which is in accordance with the particle degradation.

Our group has recently generated biodegradable nanogels based on dendritic polyglycerol via a mild and surfactant free inverse nanoprecipitation approach by CuAAC.⁴⁵ Benzacetal bonds, as the cleavable linkers, retain stability at physiological pH and enable the nanogels to efficiently degrade into small fragments under acidic conditions with a half-life of 11 h at pH 5.0 (Figure 2b). Asparaginase, which was used as a biomacromolecular protein model, was encapsulated into the protein resistant polyglycerol network with 100% efficacy and released with full enzyme activity by acid-triggered degradation of the nanogels (Figure 2c). To further understand the degradation process on the molecular scale, atomic force microscopy (AFM) was used for the real time visualization of pH-responsive nanogels based on linear- and dendritic polyglycerol with acid labile acetal bonds. As shown in Figure 15, at pH 9, the nanogels retain their size and shape due to the stable conditions for acetal bonds, whereas, decreasing the pH to 4 induces the acetal cleavage, resulting in particle erosion.¹²⁸

Figure 15. AFM images of the degradation process of polyglycerol nanogels (a-h, scan size: 5x5 μm) over time in liquid state. Picture I shows the nanogel residue in ambient conditions after degradation (scan size: 2x2 μm). Reprinted with permission from ref. 128. Copyright 2014 WILEY-VCH.

Furthermore, our group also reported the fabrication of acid-labile cell-laden microgels by combining SPAAC and droplet-based microfluidics with different substituted benzacetal linkers, which makes the degradation kinetics of microgel controllable in the pH range from 4.5 to 7.4 (Figure 3d,e,f,g).³² The encapsulated cells retained their viability while being cultured inside the microgels and could be released without detrimental effect triggered by lower pH (e.g. pH = 6.0).

The acid cleavability of benzacetals can be tuned by introducing substituents in the *para* position so that the hydrolysis kinetics can be manipulated. Fréchet et al. have developed protein-loaded hydrogels and microgels crosslinked with an acid-sensitive benzaldehyde acetal linker.⁴⁰ In their research, the bisacrylamide acetal with a *p*-methoxy substituent was chosen as the crosslinker, and achieved a rapid hydrolysis of microgels at pH 5.0 with a half-life of 5.5 min, which is much faster than other acetals.

3.1.1.2. Ketal linker

Berkland et al. have synthesized acid-labile poly(N-vinylformamide) (PNVF) nanogels through a ketal-containing crosslinker via inverse emulsion polymerization (Figure 16).¹²⁹ The encapsulation efficiency of lysozyme was affected by the ratio of monomer to crosslinker. Relatively efficient lysozyme encapsulation was obtained at the monomer-crosslinker ratio above 15, where a critical mesh size was attained. The half-life of nanogels is affected by the monomer-crosslinker ratio, e.g. at a ratio of 7, nanogels showed a half-life of 90 min at pH 5.8 compared to ~57 h at pH 7.4.

Figure 16. Synthetic approach for acid-labile PNVF nanogels. Reproduced from ref. 129. Copyright 2008 American Chemical Society.

The research group of Narain has reported thermo- and pH-sensitive biodegradable cationic nanogels based on carbohydrate as effective gene delivery carriers.²⁹ Nanogels containing a cationic thermosensitive core, which allows a facile complexation with DNA, were crosslinked with acid-cleavable linker, 2,2-dimethacroyloxy-1-ethoxypropane. The acid-cleavable property of nanogels facilitated the degradation of nanogels at endosomal pH, which intracellularly released the complexed DNA. These dual responsive nanogels presented low toxicities and high gene expression, making them potential candidates for gene expression vectors.

3.1.2. Ester

3.1.2.1. Carboxylate ester

Matyjaszewski et al. have prepared biodegradable POEO₃₀₀MA-co-PHEMA nanogel with hydrolytically labile crosslinkers by electron transfer ATRP via inverse miniemulsion.¹³⁰ They have further fabricated hyaluronic acid (HA) nanostructured hydrogel from the acryloyl chloride functionalized nanogels and thiol-derivatized HA (HA-SH) via a Michael-type addition reaction. The polyester was reported to be degradable under physiological conditions through the cleavage of the ester bond.^{131, 132} The degradable hydrogels are potential candidates for tissue engineering and cell encapsulation, while the nanogels facilitate the controlled release of small biomolecules by taking the advantage of a second delivery carrier in addition to the macroscopic matrix.

3.1.2.2. Boronate ester

Narain et al. have prepared thermo-, pH- and glucose- responsive hydrogels and nanogels via boronic-diol interaction between poly(N-isopropylacrylamide-*st*-5-methacrylamino-1,2-benzoxaborole) and the glycopolymers (Figure 9).⁹¹ The hydrogels were completely dissociated in weakly acidic solution due to the cleavage of the boronate ester as well as in excess glucose solution, because the competitive complexation of glucose molecules with benzoxaborole caused the dissociation of the

glycopolymers from the gels.

Our group has developed a boronate crosslinked nanogel system that has been introduced in Section 2.1.7 above. The nanogel swelled at pH 5 after 24 h incubation and completely degraded at pH 4. The MTX-loaded nanogel could partial release the drug in the mildly acidic environment in endo/lysosomal compartments after endocytosis, resulting from the partial cleavage of boronate ester bonds. Moreover, the electrostatic repulsion and the partial cleavage of the boronate linkages induced the swelling of the nanogel and thus facilitate the nanogel breaking up the endo/lysosomal membrane (Figure 17).⁹²

Figure 17. Intracellular pathway of MTX-loaded nanogel: (1) Passive targeting and endocytosis of nanogel, (2) acidity-induced nanogel swelling and protonation of amino groups, (3) disruption of organelle membrane, (4) endo/lysosomal membrane permeation, (5) ATP-triggered dissociation of nanogel. Reprinted with permission from ref. 92. Copyright 2014 WILEY-VCH.

3.1.2.3. Carbonate

The research group of Smedt has reported the preparation of cationic biodegradable microgels by copolymerization of dextran hydroxylethyl methacrylate (dex-HEMA) with dimethyl aminoethyl methacrylate (DMAEMA) and the incorporation of siRNA in the hydrogel network.¹³³ The carbonate ester crosslinks hydrolyzed under pH 7.4, which resulted in the release of siRNA from the microgels. They concluded that the crosslinking density can affect the degradation rate and therefore govern the siRNA release profile.

Afterwards, Smedt et al. also engineered biodegradable cationic dextran nanogels by inverse emulsion photopolymerization as potential siRNA carriers.²⁷ The degradation of dex-HEMA nanogels, which is a prerequisite for an efficient gene silencing in the absence of endosomolytic tools, showed a pH-dependent tendency with a faster hydrolysis at physiological pH than at acidic pH. With controllable degradation kinetics, the nanogels could be suitable for prolonged, time-controlled gene silencing uses.

3.1.3. Imine linker

Yang et al. fabricated composite microgel capsules by in situ surface crosslinking through benzoic-imine linkages, which are formed between the amino groups of glycol chitosan (GC) and benzaldehyde bifunctionalized poly(ethylene glycol) (OHC-PEG-CHO).³⁹ The gel capsules swell with decreasing pH due to the lability of the imine linkage at acidic pH, causing a degradation of crosslinking. Later on, they also synthesized protein nanogels by crosslinking urokinase with OHC-PEG-CHO.⁶⁵ The crosslinked structure efficiently maintained the stability of the protein by preventing the enzyme degradation, which can keep it stable under physiological conditions and dissociated at acidic pH, resulting in reversible bioactivity of the

protein in the intracellular compartments.

3.1.4. Hydrazone linker

The hydrazone linker is hydrolytically cleavable, particularly at low pH values, and the hydrolysis rate is negatively related to the pH value.¹³⁴ Degradation of the hydrazone bond is more than 10 times faster at pH 5.5 than at pH 7.4. Hydrazone linker has been used for the design of acid-degradable linear polymers, crosslinked nanoparticles, and polymer-conjugated prodrugs.^{126, 135}

Hydrazone bonds have been widely used as crosslinker in hydrogels.^{136, 137} Hoare et al. reported injectable hydrazone-crosslinked hydrogels formed by hydrazide functionalized polymer and aldehyde functionalized carbohydrate.¹³⁷ The hydrogel degradation was monitored under various concentrations of hydrochloric acid. With increasing the concentration of H⁺, the degradation rate increased, confirming that the acid-catalyzed hydrolysis of hydrazone bond is the driving force for the hydrogel degradation.

Ossipov and coworkers have constructed a hyaluronic acid (HA) hydrogel by employing the thiol-disulfide exchange reaction and carbazone chemistry. Both DOX and HA were linked to poly(vinyl alcohol) (PVA) backbone, and the release of DOX was observed more efficiently at acidic pH than neutral conditions due to the acid-cleavability of carbazone bond.¹³⁶

However, the use of hydrazone bond as the crosslinker of micro- and nanogels has not been reported yet. Besides, it has also been used as the linker between drugs and carriers, which can reduce the side effects towards normal tissues and cells and improve the efficacy in killing tumor cells due to the sufficient stability of hydrazone linker under physiological pH, whereas the efficient cleavability in acidic conditions (tumor tissue and intracellular compartments).^{135, 138, 139}

3.1.5. Vinyl ether

Thompson and Akiyoshi et al. have developed self-assembled nanogels, composed of acid-labile cholesteryl-modified pullulan (acL-CHP) via click reaction (Figure 18a,b). The hydrolysis of cholesteryl vinyl ether groups was rapid (~ 1 h) at acidic pH,¹⁴⁰⁻¹⁴² but the degradation of acL-CHP nanogels was much slower, probably due to the formation of a more stable acetal intermediate (Figure 18c), which is hydrolyzed much slower than vinyl ethers at acidic pH. The formation of acetal byproducts may have produced protein-nanogel complexes so that the release rate of the BSA cargo was slower than the hydrolysis rate of the acL-CHP nanogels under acidic conditions.¹⁴³

Figure 18. (a) Degradation of acL-CHP nanogel at acidic pH. (b) Chemical structure of acL-CHP. (c) The hypothesis of hydrolysis mechanism of cholesteryl vinyl ether group under acidic conditions. Reprinted with permission ref. 143. Copyright 2013 American Chemical Society.

3.2. Redox cleavable

In addition to pH-cleavable crosslinks, the reduction-responsive crosslinks, which make use of the redox gradients between the oxidizing extracellular medium and the reductive intracellular environments, are also well-known with regard to composing bio-responsive hydro-, micro- and nanogels.¹⁴⁴ Glutathione (GSH) tripeptide, the most abundant reducing agent in the intracellular conditions, exists in the milli-molar range (~ 1-11 mM) in the cytosol, and in the micro-molar range (~ 10 μ M) in extracellular fluids.¹⁴⁵⁻¹⁴⁸ Moreover, it has been found that the GSH level is even higher in cancer cells than in normal cells.^{149, 150} The disulfide links are stable during the blood circulation, but are efficiently cleaved under the intracellular reductive condition, which enables rapid drug release and facilitates the site-specific delivery of anti-tumor drugs in cancer therapeutics.^{125, 151}

Matyjaszewski et al. have constructed biodegradable nanogels with disulfide-functionalized dimethacrylate (DMA) crosslinkers by inverse miniemulsion atom transfer radical polymerization (ATRP).⁴⁸ The nanogels were degraded into individual polymeric chains in GSH solution, which enables both the release of encapsulated cargos and the removal of blank carriers.

Furthermore, Thayumanavan and coworkers designed disulfide crosslinked polymeric nanogels based on a oligoethyleneglycol (OEG)-containing random copolymer with pyridyl disulfide (PDS) side chains, by a simple thiol-disulfide exchange reaction without using organic solvents, metal-containing catalysts, or additional reagents.¹⁵² The stability of the noncovalent dye encapsulation inside the nanogels can be adjusted by varying the crosslinking density, which has been demonstrated by *in vitro* fluorescence resonance energy transfer (FRET) experiments. The nanogels showed favorable stability by keeping the guest molecules from leaching prior to endocytosis. The release of encapsulated DOX is triggered by GSH treatment due to the cleavage of the disulfide crosslinks, achieving drug-induced cytotoxicity to tumor cells.

These nanogels are surface functionalized with thiol-modified Tat peptide or FITC via the thiol-disulfide exchange reaction with residual PDS functionalities in the nanogels.³⁶ By using the same method, the group of Matyjaszewski functionalized the nanogels with different cysteine-modified ligands, including folic acid, cyclic arginine-glycine-aspartic acid (cRGD) peptide, and cell-penetrating peptide.³⁵ RGD- and folic acid-modified nanogels exhibit superior cellular uptake by integrin and folate receptors overexpressing cells, whereas cell-penetrating peptide-decorated nanogels result in rapid nonspecific uptake by the cells. The hydrophobic chemotherapeutic drugs can be stably encapsulated, delivered to the specific receptor-rich cells, and released inside the cells because of the cleavage of disulfide crosslinks under intracellular reductive conditions.

Zhong and coworkers developed reductive degradable nanogels depending on the *in situ* crosslinking of poly(ethylene glycol)-*b*-poly(2-(hydroxyethyl) methacrylate-co-acryloyl carbonate) (PEG-P(HEMA-co-AC)) block copolymers with cystamine via nucleophilic ring-opening reaction for intracellular protein delivery

(Figure 19).³⁴ The model protein cytochrome C (CC) was encapsulated under mild conditions with high loading and exhibited a limited immature release under physiological conditions. The proteins were released without denaturation under intracellular reductive conditions due to the de-crosslinking of the nanogels, showing better antitumor activity than free CC.

Figure 19. Schematic illustration of the formation of reduction-sensitive nanogels for protein loading and reduction-triggered release. Reprinted with permission from ref. 34. Copyright 2013 American Chemical Society.

Very recently, we developed charge-conversional and reduction-sensitive polyvinyl alcohol (PVA) nanogels for efficient cancer treatment by enhanced cell uptake and intracellular triggered doxorubicin (DOX) release. Interestingly, confocal laser scanning microscopy (CLSM) revealed that these ultra pH-sensitive nanogels could reverse their surface charge from negative to positive for improved cell internalization under a tumor extracellular pH (6.5–6.8). Furthermore, MTT assays and real time cell analysis (RTCA) showed that these DOX-loaded nanogels had a significant cell toxicity following 48 h of incubation.¹⁵³

Du and Li et al. have described the preparation of thermo-, pH-, and redox-responsive nanogels by copolymerization of monomethyl oligo(ethylene glycol) acrylate (OEGA) and 2-(5,5-dimethyl-1,3-dioxan-2-yloxy) ethyl acrylate (DMDEA), an acrylic monomer containing ortho ester, with a crosslinker bis(2-acryloyloxyethyl) disulfide (BADS) via miniemulsion.¹⁵¹ As shown in Figure 20, the cleavage of the disulfide crosslinks in these nanogels produced water-soluble polymers, which probably promotes the kidney elimination. However, single polymer chains below 20 nm were not detected by DLS after degrading the nanogels with DTT, probably owing to some unbreakable linkages formed by chain transfer to the disulfide bond in the process of radical polymerization. The hydrophobic drugs, paclitaxel (PTX)- and DOX-loaded nanogels showed good stability at physiological pH with or without serum and bio-responsive (acidic pH and redox potential) release behaviors. The PTX-loaded nanogels display concentration-dependent toxicity to tumor cells.

Figure 20. Synthetic pathway and stimuli-responsive behavior of nanogels. Reprinted with permission from ref. 151. Copyright 2011 WILEY-VCH.

We have recently developed a pH- and redox-responsive prodrug nanogel, in which DOX was conjugated via an acid-labile hydrazone linker, based on a thiol-disulfide exchange reaction by an inverse nanoprecipitation method (Figure 6).³⁸ The prodrug nanogels remained stable under physiological conditions, and the size was big enough for enhanced permeation and retention (EPR) effect in tumor tissue. These nanogels were efficiently internalized into the tumor cells by endocytosis, ending up in the endosome/lysosome, where the hydrazone linker was cleaved under decreasing pH values. Rapid release of DOX occurred as soon as the nanogels were degraded in the cytosolic reductive environment.

3.3. Photo cleavable

Photochemical reactions are easy to spatiotemporally control, in other words, the reactions can be controlled by when and where light is delivered to the systems,^{154, 155} which makes them potential cytocompatible reactions.¹⁵⁶ However, the ultraviolet light could cause the toxicity in the range of mid UV (280-315 nm) and far UV (200-280 nm). Therefore, the functional wavelength is of great importance when photochemistry is applied in the biomedical fields.

The ortho-nitrobenzyl (Figure 21) is one of the most important and useful photolabile groups in biomedical applications due to its biocompatibility and the inertia of the residues both before and after photodegradation for fragile biomacromolecules, such as proteins, DNAs, and RNAs.¹⁵⁷

Figure 21. Photodegradation of ortho-nitrobenzyl ester derivative.

Landfester et al. have reported an easy way to prepare dual-responsive microgels with photodegradable crosslinkers containing a *o*-nitrobenzylic group by inverse miniemulsion copolymerization.¹⁵⁸ The model protein myoglobin was efficiently loaded and showed a two-step release: first a slow diffusion controlled release induced by pH changes and subsequently a fast degradation controlled on-demand release induced by photo irradiation.

Zhao and coworkers have developed thermal- and photo-responsive core-shell nanogel particles based on the self-assembly of a double-hydrophilic block copolymer, containing coumarin moieties in aqueous solution.¹⁵⁹ Photodimerization of coumarin under UV irradiation ($\lambda > 310$ nm) resulted in both core- and shell-cross-linked nanogels, that exhibited photocleavage under $\lambda < 260$ nm, which caused the nanogels to swell.

3.4. Enzyme cleavable

Enzymatically degradable micro- and nanogels have been employed in biomedical applications, such as site-specific drug delivery since the enzyme concentration is cell- and tissue type-dependent, which enables the trigger of local drug release.^{42, 76, 154} The group of Wang has synthesized enzymatically cleavable nanogels, based on block copolymers containing a polyphosphoester, which undergoes hydrophobic-to-hydrophilic transition induced by salt, by a template-free method via photo-crosslinking.⁷⁶ DOX was loaded using a “breath-in” method and released with acceleration by phosphodiesterase I enzyme, which exists in mammalian cells and has been reported to catalyze the phosphoester linker degradation.

Later on, they engineered polyphosphoester core-crosslinked nanogels decorated with mannosyl ligands on the PEG shell for targeted antibiotic delivery (Figure 22a).⁴² Vancomycin, a model hydrophilic antibiotic, was loaded into the nanogels, and released after the degradation of the nanogels triggered by the active bacterial enzyme, phosphatase or phospholipase. As shown in Figure 22b, the mannosylated nanogels preferentially delivered the loaded antibiotic to macrophages and also entered into the

bacterial infection site *in vivo*, to inhibit the growth of the model bacterium, a methicillin-resistant strain of *staphylococcus aureus* (MRSA), MW2, by an enzyme-triggered release of the antibiotics vancomycin.

Figure 22. (a) The structure of vancomycin-loaded mannosylated nanogels (MNG-V) and bacteria-responsive drug release, (b) targeted uptake and transport of MNG-V, drug release, and bacteria inhibition. Reprinted with permission from ref. 42. Copyright 2012 WILEY-VCH.

3.5. Reversible click reactions

The reversible click reactions have restricted applications in biomedical field because harsh degradation conditions are required, such as high temperature,¹⁶⁰ ultrasonic,¹⁶¹ organic solvents,¹⁶² and so on. Until now, no utilization of reversible click reactions has been reported in the micro- and nanogel degradation. Herein, we only show some examples of hydrogels where these reactions have been applied.

3.5.1. Retro-Diels-Alder reaction (retro-DA reaction)

Wei et al. have synthesized thermo-sensitive hydrogels based on diene or dienophile functionalized polymers by DA-reaction under mild conditions with the advantages of initiator- or catalyst-free, organic solvent-free, tunable gelation rate, and thermal reversibility.¹⁶² The gelation occurs at low temperatures and can be accelerated by increasing the temperature. The hydrogels are stable in water even under high temperature, but are dissociable in DMF because the retro-DA reaction is accelerated by DMF.

The research group of Shoichet has designed hyaluronic acid (HA) based hydrogels from furan-modified HA and dimaleimide-decorated PEG by a one-step DA “click” reaction in aqueous solution, which showed cytocompatibility, a similar elastic modulus to the central nervous systems tissue, minimal swelling, and complete degradation.¹⁶³ All these properties make them potential candidates for soft tissue engineering.

Göpferich et al. have first reported that the degradation of hydrogels by retro-DA reactions can occur at body temperature.¹⁶⁴ Maleimide and furyl-functionalized branched PEG macromonomers were synthesized and used to prepare hydrogels by DA reactions. The hydrogel degradation, which was caused by the retro-DA reaction and the subsequent hydrolysis of maleimides to maleamic acid derivatives, was dependent on the concentration of the polymer and the type of the used macromonomers.

3.5.2. Retro-Michael addition reaction

Kiick and coworkers have investigated the degradability of the succinimide thioether formed by the thiol-maleimide Michael addition reaction, which is generally

considered a stable bond, in the presence of excess reductant at physiological conditions.¹⁶⁵ They further employed the retro-Michael addition reaction to produce hydrogels with GSH-sensitive linkages, succinimide-thioether, the cleavage of which was 10-fold slower than that of disulfide crosslinkers, which induced prolonged drug release.¹⁶⁶

3.6. Additive cleavable

Narain et al. have synthesized multi-responsive gels formed via boronic-diol interaction as discussed in Section 2.1.7 above. The crosslinked network was destroyed in glucose solution due to the glucose molecules competitively interacting with benzoxaborole, dissociating the glycopolymer from the complex.⁹¹

Adenosine-5'-triphosphate (ATP) is a multifunctional nucleotide with the intracellular concentration in the range of 1 to 10 mM, which is much higher than its extracellular concentration (< 5 μ M).¹⁶⁷ This concentration gradient was used by our group to promote the intracellular degradation of nanogels and release of drug payload (As illustrated in Section 2.1.7 and 3.1.2.2, Figure 10 and 17). In the presence of 5 mM ATP, the nanogel was dissociated into small fragments below 10 nm after 24 h, resulting in enhanced release rate of MTX.

4. Supramolecular crosslinkings and dissociation

Noncovalent interactions, such as ionic interactions, hydrophobic interactions, hydrogen bonding, or combinations thereof, can be used to physically crosslink macromolecules to obtain cell-compatible micro- and nanogels. Supramolecularly crosslinked gels afford a simple network formation without the use of any potentially toxic chemical crosslinkers or initiators. The degradation can be triggered via external stimuli by disturbing the interactions of the noncovalent crosslinks.¹⁵⁴

4.1. UV-induced dissociation

Yuan et al. have designed and synthesized a photoresponsive microgel by combining a noncovalent assembly process with a covalent crosslinking method by the host-guest interaction between azobenzene-functionalized poly(ethylene glycol) [(PEG-(Azo)₂)] and acrylate-modified β -CD (β -CD-MAA), to form a photoresponsive inclusion complex, which was crosslinked by thiol-functionalized PEG (PEG-dithiol) via Michael addition click reaction.¹⁶⁸ Upon UV irradiation at 365 nm, the spherical particles with a diameter of 200-250 nm decreased to 40-60 nm due to the photoisomerization of PEG-(Azo)₂ from trans- to cis-, inducing the dissociation of the microgel, which was still crosslinked by PEG-dithiol. The size of the microgel could return under visible light treatment at 450 nm. Therefore, the size of the microgel particles can be reversibly controlled by dissociation and association of β -CD/azobenzene inclusion complex induced by alternative irradiations of UV and visible light.

4.2. Cyclodextrin-induced dissociation

Akiyoshi et al. have started the complexation of protein with hydrogel nanoparticles by the self-assembly of cholesteryl group-bearing pullulan (CHP) to prevent protein denaturation and aggregation.^{169, 170} The dissociation of nanogels, which induces the release of protein, depends on the concentration and types of cyclodextrins used. β -CD was more effective than other CDs in dissociating the CHP nanogels¹⁷¹ induced by the formation of inclusion complexes of CD with CHP.¹⁷² They demonstrated a cell-free protein synthesis technique with nanogel-based artificial chaperones to rapidly produce proteins and improve the folding efficiency. Rhodanese was successfully expressed in the presence of the nanogel without aggregation and folded to the enzymatically active form by adding a dissociation agent like CD.¹⁰⁵

They have further fabricated an injectable hydrogel by salt-induced association of a hyaluronic acid (HA)-based anionic nanogel, which was formed by the self-assembly of cholesteryl-group-bearing HA, for the delivery of recombinant human growth hormone (rhGH) (Figure 23).¹⁰² The driving force to load protein is its hydrophobic interaction with cholesteryl groups, which can form inclusion complexes with added CD derivatives, thus dissociating the CHP nanogels to release the proteins. The salt-induced injectable hydrogel with its ability to maintain a narrow range of rhGH levels in the plasma for over one week provides an easy formulation for sustained release of therapeutic proteins.

Figure 23. The formation of HA nanogel and its solution properties. Reprinted with permission from ref. 102. Copyright 2012 WILEY-VCH.

To overcome various obstacles and achieve both spatial and temporal precision disintegration, reversible crosslinked micro- and nanogels with sophisticated structural and functional properties, which are in response to one stimulus or a combination of different stimuli, are attracting more and more attention. The internal biological stimuli, pH, redox potential, and enzyme are beneficial for self-controllable release systems in clinical trials whereas external signals like light and additives can precisely release the drug in a temporal-, spatial, and dose-controllable mode by switching on or off on demand. By taking advantage of the different stimuli's merits, the cleavable micro- and nanogels now possible in theory possess promising potential in practice.

5. Conclusions and future perspectives

In this review, we highlighted the recent progress in covalent and supramolecular crosslinking methodologies to prepare micro- and nanogels. We compiled different cleavable crosslinking strategies incorporated in them, which are mostly used in the field of biomedical applications. Covalently crosslinked gel networks can maintain adequate mechanical stability and help deliver the encapsulated payload at the targeted site by surviving the harsh in vivo conditions when adjusted in the right way.

However, the crosslinking agents often are toxic and cause unspecific interaction with the bioactive payloads. In contrast, supramolecular crosslinked networks are normally formed in aqueous solution, which avoids adverse effects, but their stability is not yet satisfying in most of the studied systems.

Up to date, the most common synthetic method for the preparation of covalently crosslinked micro- and nanogels from precursors without amphiphilicity has been emulsion or inverse emulsion polymerization, in which the surfactants are essential and must be thoroughly removed from the system. Some surfactant-free techniques, for example, inverse nanoprecipitation,^{38, 45} have been developed very recently, but the bulk production of the gel particles is yet limited. Another approach commonly used for the production of micro- and nanogels is covalent/noncovalent crosslinking of self-assembling amphiphilic polymers. These polymers, however, are often accessible only in multistep synthesis. Therefore, further effort must be made for the development of simple pathways with high productivity and mild reaction conditions.

Acknowledgments

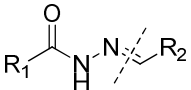
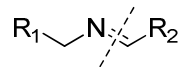
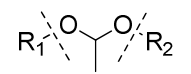
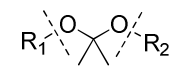
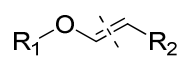
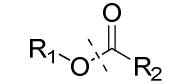
The authors would like to thank Dr. P. Winchester for proofreading this manuscript and the Chinese Scholar Council (CSC) for financial support to Xuejiao Zhang. Dr. Maria Molina acknowledges financial support from the Alexander von Humboldt Foundation. Prof. Dr. Rainer Haag is grateful to the focus area nanoscale of the Freie Universität Berlin (www.nanoscale.fu-berlin.de).

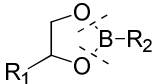
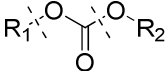
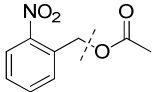
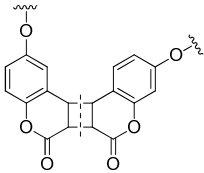
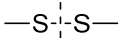
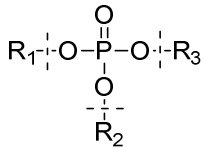
Table 1. Covalent crosslinking reactions for micro- and nanogel formation.

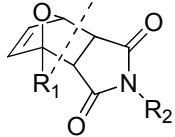
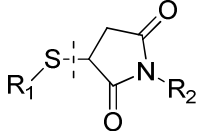
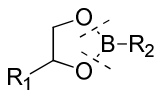
<i>Reactions</i>	<i>Reacting groups</i>	<i>Reaction conditions</i>	<i>Characterization</i>	<i>Applications</i>	
Radical polymerization	Free radical	Heating, light, or redox initiated	Formation of uniformly crosslinked network	Drug and protein delivery ⁴⁸⁻⁵²	
CuAAC	Azide and alkyne	Copper catalyzed	Fast, versatile, regiospecific, inert to biological molecules	Protein delivery, ⁴⁵ bone targeting ⁵⁷	
	SPAAC	Azide and cyclooctyne	pH 7.4	Catalyst-free, tedious synthesis	Cell encapsulation ³²
Copper free click chemistry	Thiol-ene	Thiol and unsaturated groups (alkenes)	Radical initiated (photo-irradiation)	Spatiotemporal control	Drug delivery, ¹⁷³ dye separation ⁶¹
	Michael addition	Thiol and α , β -unsaturated carbonyl group (acrylates and maleimides)	pH 6-8, no catalyst	Fast reaction kinetics	Template for mesoporous silica synthesis ⁶⁴

Schiff-base reaction	Aldehyde and amine or hydrazide	no catalyst	Mild reaction conditions	Protein delivery, ⁶⁵ functional surface ⁶⁶
Thiol-disulfide exchange reaction	Thiol and disulfide	pH > 8	Mild reaction condition, ease of further functionalization	Drug and protein delivery ^{35-37, 43, 71-73}
Photo-induced crosslinking	Coumarin or alkene	UV irradiation, photo initiator	Highly efficient, cytotoxicity issues	Drug delivery ¹⁷⁴
Amide-based crosslinking	Amine and carboxylic acids or activated ester	No additive needed	Adjustable crosslinking degree	Drug and protein delivery ^{79, 80}
Boronic-diol complexation	Boronic acid and diols	pH > pK _a of boronic acid	Formation of dissociable complexation	Cell encapsulation ⁹⁰
Enzyme-catalyzed crosslinking	Thiol	HRP catalyzed	No H ₂ O ₂ needed	Cell and protein encapsulation ⁹⁶
Siloxane crosslinking	Siloxane	Heating or acidic condition	Formation of base-labile Si-O-Si bond, harsh reaction conditions	No applications in biomedical fields

Table 2. Labile crosslinkers used in degradable micro- and nanogels.

crosslinkers	structure	Cleavable conditions	Reference
Acid-cleavable			
Hydrazone linker		pH 5.5, 100 % degradation within 200 min, 10 times faster than pH 7.5	126, 134, 135
Imine linker		pH 5, cleavable within 3 h	65
Acetal linker		Bisacrylamide acetal with a p-methoxy substituent, pH 5, half-life 5.5 min; slightly acidic pH, complete hydrolysis < 1 h	32, 127
Ketal linker		pH 5.5, half-life 2 h	175
Vinyl ether		Hydrolysis at pH < 5	143
Carboxylate ester		Hydrolysis under physiological conditions	130

Boronate ester		pH 5, cleavage in 120 min	88, 89, 176
Carbonate		Complete degradation under physiological conditions after 6 days	26
Photo-cleavable			
Ortho-nitrobenzyl ester		UV 315-390 nm	158
Biscoumarin		UV < 260 nm	74
Redox-cleavable			
Disulfide		DTT, TCEP, GSH	35, 36, 38, 48, 73, 101, 151, 152
Enzyme-cleavable			
phosphoester		Phosphatase, phospholipase	42, 76

Reversible click reactions			
Retro-Diels-Alder		DMF can accelerate retro-DA reaction; Degradation by retro-DA reaction first at body temperature.	162, 164
Retro-Michael addition		GSH, 10 times slower than disulfide crosslinks	165, 166
Additive-induced dissociation			
Boronate ester		glucose	91
Cholesteryl-induce assembly	—	cyclodextrin	102, 105, 137, 170, 171

References

1. J. K. Oh, R. Drumright, D. J. Siegart and K. Matyjaszewski, *Prog. Polym. Sci.*, 2008, **33**, 448.
2. Y. Sasaki and K. Akiyoshi, *Chem. Rec.*, 2010, **10**, 366.
3. S. Seiffert, *Angew. Chem. Int. Ed.*, 2013, **52**, 11462.
4. J. K. Oh, D. I. Lee and J. M. Park, *Prog. Polym. Sci.*, 2009, **34**, 1261.
5. A. L. Sisson, D. Steinhilber, T. Rossow, P. Welker, K. Licha and R. Haag, *Angew. Chem. Int. Ed.*, 2009, **48**, 7540.
6. T. Xing, C. Mao, B. Lai and L. Yan, *ACS Appl. Mater. Interfaces*, 2012, **4**, 5662.
7. Y. W. Noh, S. H. Kong, D. Y. Choi, H. S. Park, H. K. Yang, H. J. Lee, H. C. Kim, K. W. Kang, M. H. Sung and Y. T. Lim, *ACS Nano*, 2012, **6**, 7820.
8. U. Hasegawa, S.-i. M. Nomura, S. C. Kaul, T. Hirano and K. Akiyoshi, *Biochem. Biophys. Res. Co.*, 2005, **331**, 917.
9. H. S. Park, J. E. Lee, M. Y. Cho, J. H. Hong, S. H. Cho and Y. T. Lim, *Macromol. Rapid Commun.*, 2012, **33**, 1549.
10. W. Wu, J. Shen, P. Banerjee and S. Zhou, *Biomaterials*, 2010, **31**, 7555.
11. M. Oishi, A. Tamura, T. Nakamura and Y. Nagasaki, *Adv. Funct. Mater.*, 2009, **19**, 827.
12. W. Wu, T. Zhou, A. Berliner, P. Banerjee and S. Zhou, *Chem. Mater.*, 2010, **22**, 1966.
13. W. Wu, J. Shen, Y. Li, H. Zhu, P. Banerjee and S. Zhou, *Biomaterials*, 2012, **33**, 7115.
14. W. Wu, N. Mitra, E. C. Y. Yan and S. Zhou, *ACS Nano*, 2010, **4**, 4831.
15. C. Li and S. Liu, *J. Mater. Chem.*, 2010, **20**, 10716.
16. H. Zhu, Y. Li, R. Qiu, L. Shi, W. Wu and S. Zhou, *Biomaterials*, 2012, **33**, 3058.
17. W. Wu, J. Shen, Z. Gai, K. Hong, P. Banerjee and S. Zhou, *Biomaterials*, 2011, **32**, 9876.
18. H. Peng, J. A. Stolwijk, L. Sun, J. Wegener and O. S. Wolfbeis, *Angew. Chem. Int. Ed.*, 2010, **49**, 4246.
19. W. Wu, J. Shen, P. Banerjee and S. Zhou, *Biomaterials*, 2010, **31**, 8371.
20. W. Wu, M. Aiello, T. Zhou, A. Berliner, P. Banerjee and S. Zhou, *Biomaterials*, 2010, **31**, 3023.
21. C. Zhao, Q. Chen, K. Patel, L. Li, X. Li, QiumingWang, G. Zhang and J. Zheng, *Soft Matter*, 2012, **8**, 7848.
22. A. W. Bridges, N. Singh, K. L. Burns, J. E. Babensee, L. A. Lyon and A. J. García, *Biomaterials*, 2008, **29**, 4605.
23. W. H. Blackburn, E. B. Dickerson, M. H. Smith, J. F. McDonald and L. A. Lyon, *Bioconjugate Chem.*, 2009, **20**, 960.
24. H. Mimi, K. M. Ho, Y. S. Siu, A. Wu and P. Li, *J. Control. Release*, 2012, **158**, 123.
25. A. Tamura, M. Oishi and Y. Nagasaki, *Biomacromolecules*, 2009, **10**, 1818.
26. K. Raemdonck, T. G. V. Thienen, R. E. Vandenbroucke, N. N. Sanders, J. Demeester and S. C. D. Smedt, *Adv. Funct. Mater.*, 2008, **18**, 993.
27. K. Raemdonck, B. Naeye, K. Buyens, R. E. Vandenbroucke, A. Høgset, J. Demeester and S. C. D. Smedt, *Adv. Funct. Mater.*, 2009, **19**, 1406.
28. B. Naeye, H. Deschout, M. Röding, M. Rudemo, J. Delanghe, K. Devreese, J. Demeester, K. Braeckmans, S. C. D. Smedt and K. Raemdonck, *Biomaterials*, 2011, **32**, 9120.
29. R. Sunasee, P. Wattanaarsakit, M. Ahmed, F. B. Lollmahomed and R. Narain, *Bioconjugate Chem.*, 2012, **23**, 1925.

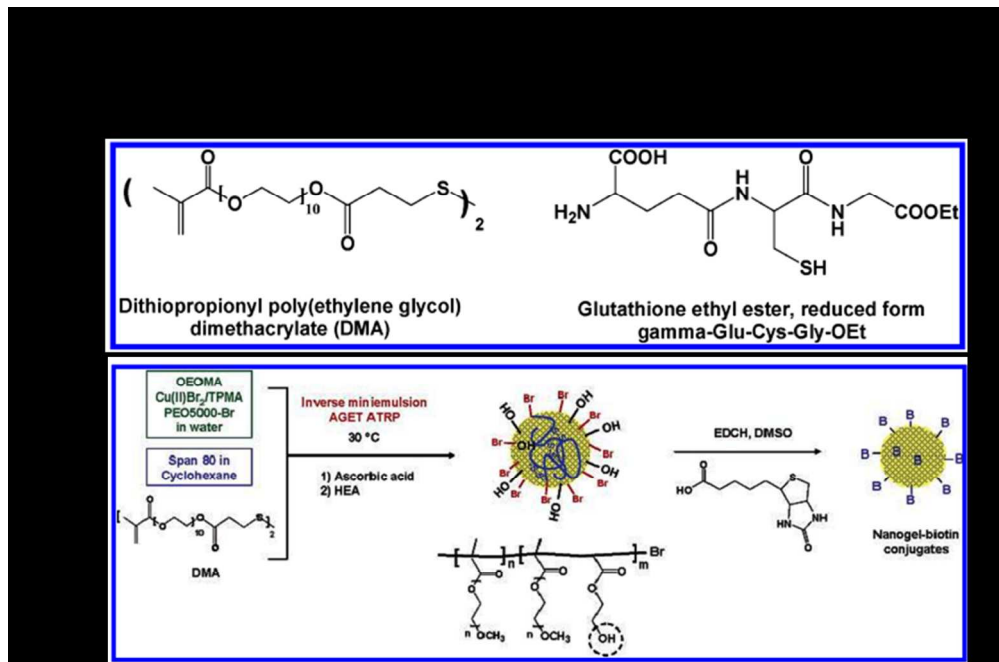
30. M. Ahmed and R. Narain, *Mol. Pharmaceutics*, 2012, **9**, 3160.
31. M. Fujioka-Kobayashi, M. S. Ota, A. Shimoda, K.-i. Nakahama, K. Akiyoshi, Y. Miyamoto and S. Iseki, *Biomaterials*, 2012, **33**, 7613.
32. D. Steinhilber, T. Rossow, S. Wedepohl, F. Paulus, S. Seiffert and R. Haag, *Angew. Chem. Int. Ed.*, 2013, **52**, 13538.
33. Y. Xia, X. He, M. Cao, C. Chen, H. Xu, F. Pan and J. R. Lu, *Biomacromolecules*, 2013, **14**, 3615.
34. W. Chen, M. Zheng, F. Meng, R. Cheng, C. Deng, J. Feijen and Z. Zhong, *Biomacromolecules*, 2013, **14**, 1214.
35. J. H. Ryu, S. Bickerton, J. Zhuang and S. Thayumanavan, *Biomacromolecules*, 2012, **13**, 1515.
36. J. H. Ryu, S. Jiwanich, R. Chacko, S. Bickerton and S. Thayumanavan, *J. Am. Chem. Soc.*, 2010, **132**, 8246.
37. K. C. R. Bahadur and P. Xu, *Adv. Mater.*, 2012, **24**, 6479.
38. X. Zhang, K. Achazi, D. Steinhilber, F. Kratz, J. Dervede and R. Haag, *J. Control. Release*, 2014, **174**, 209.
39. L. Zhao, L. Zhu, Q. Wang, J. Li, C. Zhang, J. Liu, X. Qu, G. He, Y. Lu and Z. Yang, *Soft Matter*, 2011, **7**, 6144.
40. N. Murthy, Y. X. Thng, S. Schuck, M. C. Xu and J. M. J. Fréchet, *J. Am. Chem. Soc.*, 2002, **124**, 12398.
41. V. X. Truong, M. P. Ablett, H. T. J. Gilbert, J. Bowen, S. M. Richardson, J. A. Hoyland and A. P. Dove, *Biomater. Sci.*, 2014, **2**, 167.
42. M. Xiong, Y. Li, Y. Bao, X. Yang, B. Hu and J. Wang, *Adv. Mater.*, 2012, **24**, 6175.
43. J. Zhang, F. Yang, H. Shen and D. Wu, *ACS Macro Lett.*, 2012, **1**, 1295.
44. J. K. Oh, S. A. Bencherif and K. Matyjaszewski, *Polymer*, 2009, **50**, 4407.
45. D. Steinhilber, M. Witting, X. Zhang, M. Staegemann, F. Paulus, W. Friess, S. Küchler and R. Haag, *J. Control. Release*, 2013, **169**, 289.
46. N. Sansona and J. Rieger, *Polym. Chem.*, 2010, **1**, 965.
47. J. Ramos, J. Forcada and R. Hidalgo-Alvarez, *Chem. Rev.*, 2014, **114**, 367.
48. J. K. Oh, D. J. Siegwart, H.-i. Lee, G. Sherwood, L. Peteanu, J. O. Hollinger, K. Kataoka and K. Matyjaszewski, *J. Am. Chem. Soc.*, 2007, **129**, 5939.
49. D. J. Siegwart, A. Srinivasan, S. A. Bencherif, A. Karunanidhi, J. K. Oh, S. Vaidya, R. Jin, J. O. Hollinger and K. Matyjaszewski, *Biomacromolecules*, 2009, **10**, 2300.
50. S. E. Averick, A. J. D. Magenau, A. Simakova, B. F. Woodman, A. Seong, R. A. Mehl and K. Matyjaszewski, *Polym. Chem.*, 2011, **2**, 1476.
51. L. Yan and W. Tao, *Polymer*, 2010, **51**, 2161.
52. N. Bhuchar, R. Sunasee, K. Ishihara, T. Thundat and a. R. Narain, *Bioconjugate Chem.*, 2012, **23**, 75.
53. H. C. Kolb, M. G. Finn and K. B. Sharpless, *Angew. Chem. Int. Ed.*, 2001, **40**, 2004.
54. M. G. Finn and V. V. Fokin, *Chem. Soc. Rev.*, 2010, **39**, 1231.
55. A. L. Sisson and R. Haag, *Soft Matter*, 2010, **6**, 4968.
56. A. L. Sisson, I. Papp, K. Landfester and R. Haag, *Macromolecules*, 2009, **42**, 556.
57. D. A. Heller, Y. Levi, J. M. Pelet, J. C. Doloff, J. Wallas, G. W. Pratt, S. Jiang, G. Sahay, A. Schroeder, J. E. Schroeder, Y. Chyan, C. Zurenko, W. Queres, M. Manzano, D. S. Kohane, R. Langer and D. G. Anderson, *Adv. Mater.*, 2013, **25**, 1449.
58. Y. Jiang, J. Chen, C. Deng, E. J. Suuronen and Z. Zhong, *Biomaterials*, 2014, **35**, 4969.

59. J. C. Jewett and C. R. Bertozzi, *Chem. Soc. Rev.*, 2010, **39**, 1272.
60. J. Xu, T. M. Fillion, F. Prifti and J. Song, *Chem. Asian J.*, 2011, **6**, 2730.
61. B. Li, X. Jiang and J. Yin, *J. Mater. Chem.*, 2012, **22**, 17976.
62. B. D. Mather, K. Viswanathan, K. M. Miller and T. E. Long, *Prog. Polym. Sci.*, 2006, **31**, 487.
63. T. Rossow, J. A. Heyman, A. J. Ehrlicher, A. Langhoff, D. A. Weitz, R. Haag and S. Seiffert, *J. Am. Chem. Soc.*, 2012, **134**, 4983.
64. Y. Li, J. Yang, W. Wu, X. Zhang and R. Zhuo, *Langmuir*, 2009, **25**, 1923.
65. H. Tan, H. Jin, H. Mei, L. Zhu, W. Wei, Q. Wang, F. Liang, C. Zhang, J. Li, X. Qu, D. Shangguan, Y. Huang and Z. Yang, *Soft Matter*, 2012, **8**, 2644.
66. E. Faure, C. Falentin-Daudré, T. S. Lanero, C. Vreuls, G. Zocchi, C. V. D. Weerd, J. Martial, C. Jérôme, A.-S. Duwez and C. Detrembleur, *Adv. Funct. Mater.*, 2012, **22**, 5271.
67. C. S. Sevier and C. A. Kaiser, *Nat. Rev. Mol. Cell Biol.*, 2002, **3**, 836.
68. Y. Li, L. Zhu, Z. Liu, R. Cheng, F. Meng, J. Cui, S. Ji and Z. Zhong, *Angew. Chem. Int. Ed.*, 2009, **48**, 9914.
69. U. Singh and I. Jialal, *Nutr. Rev.*, 2008, **66**, 646.
70. J. Bustamante, J. K. Lodge, L. Marcocci, H. J. Tritschler, L. Packer and B. H. Rihn, *Free Radical Bio. Med.*, 1998, **24**, 1023.
71. L. Li, K. Raghupathi, C. Yuan and S. Thayumanavan, *Chem. Sci.*, 2013, **4**, 3654.
72. S. Bickerton, S. Jiwpanich and S. Thayumanavan, *Mol. Pharmaceutics*, 2012, **9**, 3569.
73. D. C. Gonzalez-Toro, J.-H. Ryu, R. T. Chacko, J. Zhuang and S. Thayumanavan, *J. Am. Chem. Soc.*, 2012, **134**, 6964.
74. J. He, B. Yan, L. Tremblay and Y. Zhao, *Langmuir*, 2011, **27**, 436.
75. J. He, X. Tong and Y. Zhao, *Macromolecules*, 2009, **42**, 4845.
76. Y. Wang, Juan Wu, Y. Li, J. Du, Y. Yuan and J. Wang, *Chem. Commun.*, 2010, **46**, 3520.
77. C. G. Williams, A. N. Malik, T. K. Kim, P. N. Manson and J. H. Elisseeff, *Biomaterials*, 2005, **26**, 1211.
78. R. T. Chacko, J. Ventura, J. Zhuang and S. Thayumanavan, *Adv. Drug Deliver. Rev.*, 2012, **64**, 836.
79. J. Zhuang, S. Jiwpanich, V. D. Deepak and S. Thayumanavan, *ACS Macro Lett.*, 2012, **1**, 175.
80. C. W. Park, H. M. Yang, H. J. Lee and J. D. Kim, *Soft Matter*, 2013, **9**, 1781.
81. M. A. Pujana, L. Pérez-Álvarez, L. C. C. Iturbe and I. Katime, *Polymer*, 2012, **53**, 3107.
82. M. Piest, X. Zhang, J. Trinidad and J. F. J. Engbersen, *Soft Matter*, 2011, **7**, 11111.
83. A. Mahalingam, J. I. Jay, K. Langheinrich, S. Shukair, M. D. McRaven, L. C. Rohan, B. C. Herold, T. J. Hope, P. F. Kiser and M. P. Ablett, *Biomaterials*, 2011, **32**, 8343.
84. J. I. Jay, S. Shukair, K. Langheinrich, M. C. Hanson, G. C. Cianci, T. J. Johnson, M. R. Clark, T. J. Hope and P. F. Kiser, *Adv. Funct. Mater.*, 2009, **19**, 2969.
85. M. C. Roberts, M. C. Hanson, A. P. Massey, E. A. Karren and P. F. Kiser, *Adv. Mater.*, 2007, **19**, 2503.
86. L. He, D. E. Fullenkamp, J. G. Rivera and P. B. Messersmith, *Chem. Commun.*, 2011, **47**, 7497.
87. J. Xu, D. Yang, W. Li, Y. Gao, H. Chen and H. Li, *Polymer*, 2011, **52**, 4268.
88. W. Chen, Y. Cheng and B. Wang, *Angew. Chem. Int. Ed.*, 2012, **51**, 5293.
89. Y. Li, W. Xiao, K. Xiao, L. Berti, J. Luo, H. P. Tseng, G. Fung and K. S. Lam, *Angew. Chem. Int. Ed.*, 2012, **51**, 2864.
90. T. Aikawa, T. Konno, M. Takai and K. Ishihara, *Langmuir*, 2011, **28**, 2145.

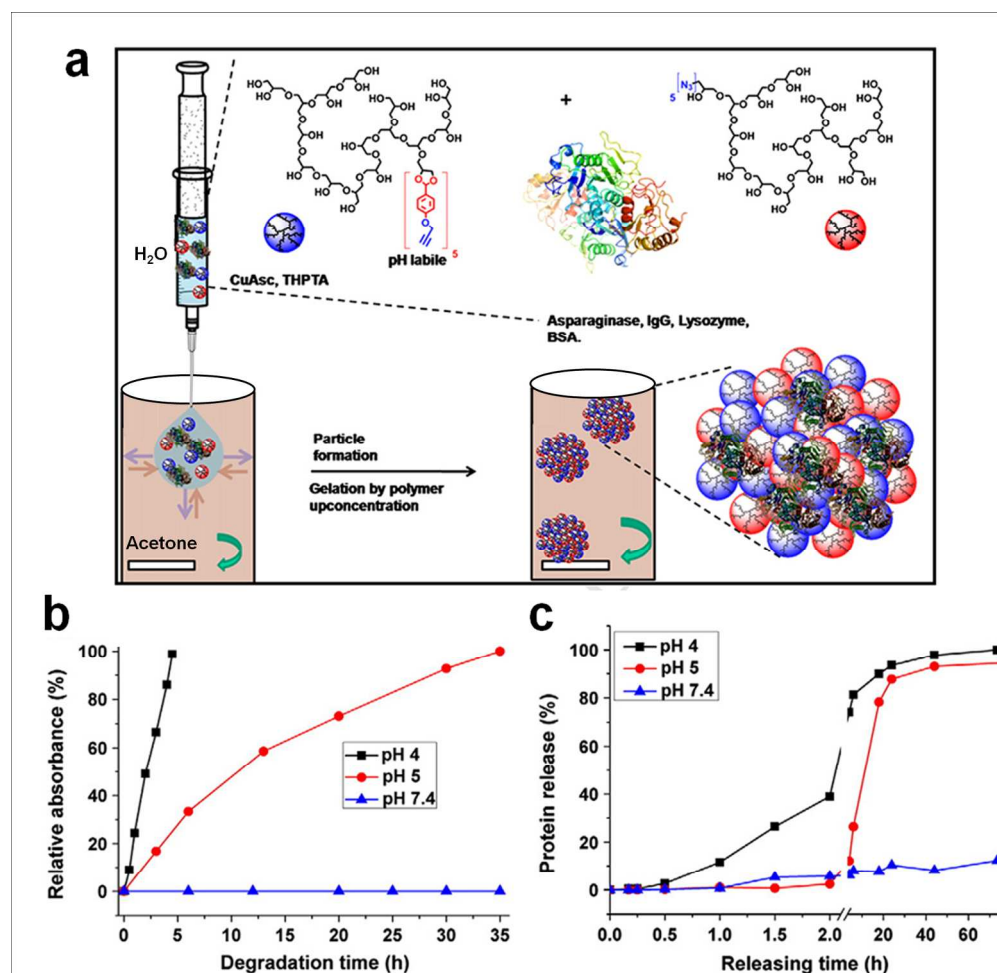
91. Y. Kotsuchibashi, R. V. C. Agustin, J. Y. Lu, D. G. Hall and R. Narain, *ACS Macro Lett.*, 2013, **2**, 260.
92. X. Zhang, K. Achazi and R. Haag, *Adv. Healthc. Mater.*, 2014, DOI: 10.1002/adhm.201400550.
93. D. J. Menzies, A. Cameron, T. Munro, E. Wolvetang, L. Grøndahl and J. J. Cooper-White, *Biomacromolecules*, 2012, **14**, 413.
94. K. M. Park, Y. Lee, J. Y. Son, J. W. Bae and K. D. Park, *Bioconjugate Chem.*, 2012, **23**, 2042.
95. R. DeVolder, E. Antoniadou and H. Kong, *J. Control. Release*, 2013, **172**, 30.
96. S. Singh, F. Topuz, K. Hahn, K. Albrecht and J. Groll, *Angew. Chem. Int. Ed.*, 2013, **52**, 3000.
97. C. Wu, C. Strehmel, K. Achazi, L. Chiappisi, J. Dervede, M. C. Lensen, M. Gradzielski, M. B. Ansoerge-Schumacher and R. Haag, *Biomacromolecules*, 2014.
98. J. Zhang, X. Liu, A. Fahr and K. D. Jandt, *Colloid Polym Sci*, 2008, **286**, 1209.
99. J. Zhang, C. Pan, T. Keller, R. Bhat, M. Gottschaldt, U. S. Schubert and K. D. Jandt, *Macromol. Mater. Eng.*, 2009, **294**, 396
100. L. S. M. Teixeira, J. Feijen, C. A. v. Blitterswijk, P. J. Dijkstra and M. Karperien, *Biomaterials*, 2012, **33**, 1281.
101. K. Kim, B. Bae, Y. J. Kang, J.-M. Nam, S. Kang and J.-H. Ryu, *Biomacromolecules*, 2013, **14**, 3515.
102. T. Nakai, T. Hirakura, Y. Sakurai, T. Shimoboji, M. Ishigai and K. Akiyoshi, *Macromol. Biosci.*, 2012, **12**, 475.
103. U. Hasegawa, S.-i. Sawada, T. Shimizu, T. Kishida, E. Otsuji, O. Mazda and K. Akiyoshi, *J. Control. Release*, 2009, **140**, 312.
104. T. Hirakura, K. Yasugi, T. Nemoto, M. Sato, T. Shimoboji, Y. Aso, N. Morimoto and K. Akiyoshi, *J. Control. Release*, 2010, **142**, 483.
105. Y. Sasaki, W. Asayama, T. Niwa, S.-i. Sawada, T. Ueda, H. Taguchi and K. Akiyoshi, *Macromol. Biosci.*, 2011, **11**, 814.
106. A. Shimoda, S.-i. Sawada and K. Akiyoshi, *Macromol. Biosci.*, 2011, **11**, 882.
107. Y. Sekine, Y. Moritani, T. Ikeda-Fukazawa, Y. Sasaki and K. Akiyoshi, *Adv. Healthc. Mater.*, 2012, **1**, 722.
108. K. Akiyoshi, S. Deguchi, H. Tajima, T. Nishikawa and J. Sunamoto, *Macromolecules*, 1997, **30**, 857.
109. K. Akiyoshi, S. Deguchi, N. Moriguchi, S. Yamaguchi and J. Sunamoto, *Macromolecules*, 1993, **26**, 3062.
110. R. Gref, C. Amiel, K. Molinard, S. Daoud-Mahammed, B. Sébille, B. Gillet, J.-C. Beloeil, C. Ringard, V. Rosilio, J. Poupaert and P. Couvreur, *J. Control. Release*, 2006, **111**, 316.
111. S. Daoud-Mahammed, P. Couvreur and R. Gref, *Int. J. Pharm.*, 2007, **332**, 185.
112. J. Lee, C. Lee, T. H. Kim, E. S. Lee, B. S. Shin, S.-C. Chi, E.-S. Park, K. C. Lee and Y. S. Youn, *J. Control. Release*, 2012, **161**, 728.
113. M. E. Davis, J. E. Zuckerman, C. H. J. Choi, D. Seligson, A. Tolcher, C. A. Alabi, Y. Yen, J. D. Heidel and A. Ribas, *Nature*, 2010, **464**, 1067.
114. K. H. Bae, H. Mok and T. GwanPark, *Biomaterials*, 2008, **29**, 3376.
115. H. Jia, H. Wang, C. Liu, C. Li, J. Yang, X. Xu, J. Feng, X. Zhang and R. Zhuo, *Soft Matter*, 2012, **8**, 6906.
116. T. Rossow, S. Hackelbusch, P. van Assenbergh and S. Seiffert, *Polym. Chem.*, 2013, **4**, 2515.
117. S. Hackelbusch, T. Rossow, H. Becker and S. Seiffert, *Macromolecules*, 2014, **47**, 4028.

118. T. Rossow and S. Seiffert, *Polym. Chem.*, 2014, **5**, 3018.
119. T. Rossow, A. Habicht and S. Seiffert, *Macromolecules*, 2014, **47**, 6473.
120. T. Rossow, S. Bayer, R. Albrecht, C. C. Tzschucke and S. Seiffert, *Macromol. Rapid Commun.*, 2013, **34**, 1401.
121. G. R. Whittell, M. D. Hager, U. S. Schubert and I. Manners, *Nat. Mater.*, 2011, **10**, 176.
122. S. Bode, L. Zedler, F. H. Schacher, B. Dietzek, M. Schmitt, J. Popp, M. D. Hager and U. S. Schubert, *Adv. Mater.*, 2013, **25**, 1634.
123. C. Fasting, C. A. Schalley, M. Weber, O. Seitz, S. Hecht, B. Kocsch, J. Dervede, C. Graf, E.-W. Knapp and R. Haag, *Angew. Chem. Int. Ed.*, 2012, **51**, 10472.
124. E. Fleige, M. A. Quadir and R. Haag, *Adv. Drug Deliver. Rev.*, 2012, **64**, 866.
125. H. Wei, R. Zhuo and X. Zhang, *Prog. Polym. Sci.*, 2013, **38**, 503.
126. S. Binauld, W. Scarano and M. H. Stenzel, *Macromolecules*, 2012, **45**, 6989.
127. V. Bulmus, Y. Chan, Q. Nguyen and H. L. Tran, *Macromol. Biosci.*, 2007, **7**, 446.
128. M. Richter, D. Steinhilber, R. Haag and R. von Klitzing, *Macromol. Rapid Commun.*, 2014, **35**, 2018.
129. L. Shi, S. Khondee, T. H. Linz and C. Berkland, *Macromolecules*, 2008, **41**, 6546.
130. S. A. Bencherif, N. R. Washburn and K. Matyjaszewski, *Biomacromolecules*, 2009, **10**, 2499.
131. S. A. Bencherif, A. Srinivasan, J. A. Sheehan, L. M. Walker, C. Gayathri, R. Gil, J. O. Hollinger, K. Matyjaszewski and N. R. Washburn, *Acta Biomater.*, 2009, **5**, 1872.
132. S. A. Bencherif, J. A. Sheehan, J. O. Hollinger, L. M. Walker, K. Matyjaszewski and N. R. Washburn, *J. Biomed. Mater. Res. A*, 2009, **90A**, 142.
133. K. Raemdonck, T. G. V. Thienen, R. E. Vandenbroucke, N. N. Sanders, J. Demeester and S. C. D. Smedt, *Adv. Funct. Mater.*, 2008, **18**, 993.
134. X. Duan, J. Xiao, Q. Yin, Z. Zhang, H. Yu, S. Mao and Y. Li, *ACS Nano*, 2013, **7**, 5858.
135. M. Calderón, P. Welker, K. Licha, I. Fichtner, R. Graeser, R. Haag and F. Kratz, *J. Control. Release*, 2011, **151**, 295.
136. D. Ossipov, S. Kootala, Z. Yi, X. Yang and J. Hilborn, *Macromolecules*, 2013, **46**, 4105.
137. M. Patenaude and T. Hoare, *Biomacromolecules*, 2012, **13**, 369.
138. W. Xiong, W. Wang, Y. Wang, Y. Zhao, H. Chen, H. Xu and X. Yang, *Colloids Surf. B Biointerfaces*, 2011, **84**, 447.
139. F. Zhan, W. Chen, Z. Wang, W. Lu, R. Cheng, C. Deng, F. Meng, H. Liu and Z. Zhong, *Biomacromolecules*, 2011, **12**, 3612.
140. J. A. Boomer and D. H. Thompson, *Chem. Phys. Lipids*, 1999, **99**, 145.
141. H. K. Kim, J. V. d. Bossche, S. H. Hyun and D. H. Thompson, *Bioconjugate Chem.*, 2012, **23**, 2071.
142. J. Shin, P. Shum, J. Grey, S.-i. Fujiwara, G. S. Malhotra, A. González-Bonet, S.-H. Hyun, E. Moase, T. M. Allen and D. H. Thompson, *Mol. Pharmaceutics*, 2012, **9**, 3266.
143. N. Morimoto, S. Hirano, H. Takahashi, S. Loethen, D. H. Thompson and K. Akiyoshi, *Biomacromolecules*, 2012, **14**, 56.
144. G. Saito, J. A. Swanson and K.-D. Lee, *Adv. Drug Deliver. Rev.*, 2003, **55**, 199.
145. J. B. Mitchell and A. Russo, *Br. J. Cancer*, 1987, **8**, 96.
146. F. Q. Schafer and G. R. Buettner, *Free Radical Bio. Med.*, 2001, **30**, 1191.
147. R. Franco and J. A. Cidlowski, *Cell Death Differ.*, 2009, **16**, 1303.
148. J. M. Estrela, A. Ortega and E. Obrador, *Crit. Rev. Cl. Lab. Sci.*, 2006, **43**, 143.

149. A. Russo, W. DeGraff, N. Friedman and J. B. Mitchell, *Cancer Res.*, 1986, **46**, 2845.
150. A. Gupte and R. J. Mumper, *Cancer Treat. Rev.*, 2009, **35**, 32.
151. Z. Qiao, R. Zhang, F. Du, D. Liang and Z. Li, *J. Control. Release*, 2011, **152**, 57.
152. J. H. Ryu, R. T. Chacko, S. Jiwanich, S. Bickerton, R. P. Babu and S. Thayumanavan, *J. Am. Chem. Soc.*, 2010, **132**, 17227.
153. W. Chen, K. Achazi, B. Schade and R. Haag, *J. Control. Release*, <http://dx.doi.org/10.1016/j.jconrel.2014.11.012>.
154. P. M. Kharkar, K. L. Kiick and A. M. Kloxin, *Chem. Soc. Rev.*, 2013, **42**, 7335.
155. C. N. Bowman and C. J. Kloxin, *AIChE J.*, 2008, **54**, 2775.
156. C. A. DeForest and K. S. Anseth, *Nat. Chem.*, 2011, **3**, 925.
157. I. Tomatsu, K. Peng and A. Kros, *Adv. Drug Deliver. Rev.*, 2011, **63**, 1257.
158. D. Klinger and K. Landfester, *Macromolecules*, 2011, **44**, 9758.
159. J. He, B. Yan, L. Tremblay and Y. Zhao, *Langmuir*, 2010, **27**, 436.
160. M. Marref, N. Mignard, C. Jegat, M. Taha, M. Belbachir and R. Meghabar, *Polym. Int.*, 2013, **62**, 87.
161. J. N. Brantley, K. M. Wiggins and C. W. Bielawski, *Science*, 2011, **333**, 1606.
162. H. Wei, Z. Yang, L. Zheng and Y. Shen, *Polymer*, 2009, **50**, 2836.
163. C. M. Nimmo, S. C. Owen and M. S. Shoichet, *Biomacromolecules*, 2011, **12**, 824.
164. S. Kirchhof, F. P. Brandl, N. Hammer and A. M. Goepferich, *J. Mater. Chem. B*, 2013, **1**, 4855.
165. A. D. Baldwin and K. L. Kiick, *Bioconjugate Chem.*, 2011, **22**, 1946.
166. A. D. Baldwin and K. L. Kiick, *Polym. chem.*, 2013, **4**, 133.
167. M. W. Gorman, E. O. Feigl and C. W. Buffington, *Clin. Chem.*, 2007, **53**, 2318.
168. H. Zhang, Y. Xin, Q. Yan, L. Zhou, L. Peng and J. Yuan, *Macromol. Rapid Commun.*, 2012, **33**, 1952.
169. Y. Nomura, M. Ikeda, N. Yamaguchi, Y. Aoyama and K. Akiyoshi, *FEBS Lett.*, 2003, **553**, 271.
170. K. Akiyoshi, Y. Sasaki and J. Sunamoto, *Bioconjugate Chem.*, 1999, **10**, 321.
171. Y. Nomura, Y. Sasaki, M. Takagi, T. Narita, Y. Aoyama and K. Akiyoshi, *Biomacromolecules*, 2004, **6**, 447.
172. S.-i. Sawada, Y. Sasaki, Y. Nomura and K. Akiyoshi, *Colloid Polym. Sci.*, 2011, **289**, 685.
173. L. Zhao, C. Xiao, J. Ding, P. He, Z. Tang, X. Pang, X. Zhuang and X. Chen, *Acta Biomater.*, 2013, **9**, 6535.
174. Y. Wang, J. Wu, Y. Li, J. Du, Y. Yuan and J. Wang, *Chem Commun*, 2010, **46**, 3520.
175. R. A. Shenoi, B. F. L. Lai and J. N. Kizhakkedathu, *Biomacromolecules*, 2012, **13**, 3018.
176. L. Li, Z. Bai and P. A. Levkin, *Biomaterials*, 2013, **34**, 8504.

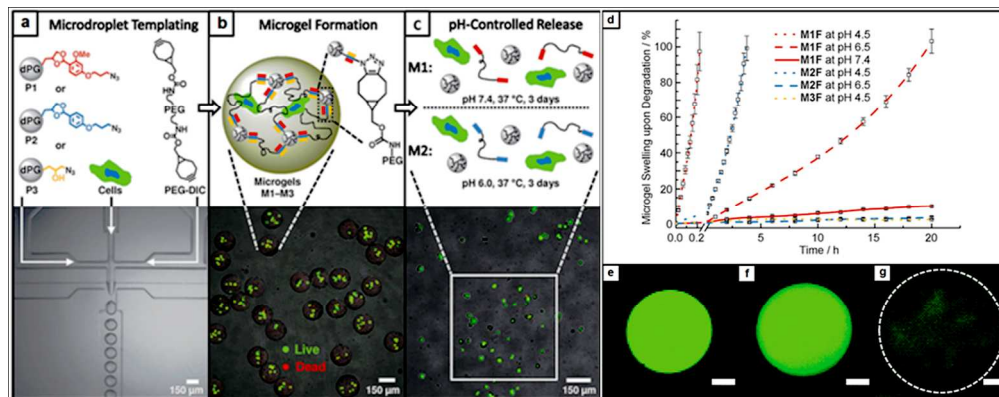


(a) Chemical structures of the crosslinker DMA and glutathione ethyl ester. (b) Synthesis of biodegradable nanogels by ATRP and functionalization of nanogels with biotin. Reprinted with permission from ref. 48. Copyright 2007 American Chemical Society. 254x167mm (150 x 150 DPI)



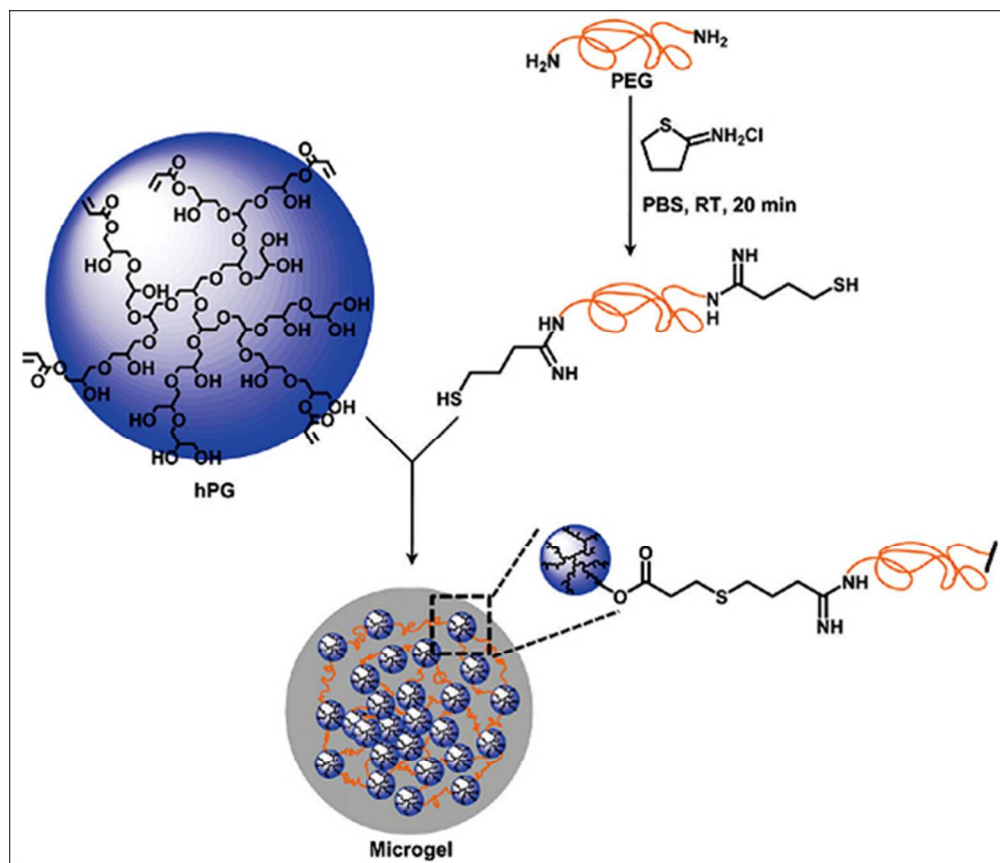
(a) Reverse nanoprecipitation process for nanogel formation. Injection of an aqueous solution of azide functionalized polyglycerol (red spheres), alkyne functionalized polyglycerol (blue spheres), and a 3D protein structure. Formation of a particle template after the aqueous phase diffused into the acetone phase. Crosslinking by CuAAC is achieved due to upconcentration. (b) Degradation of polyglycerol nanogels at different pH determined by UV/vis absorption. (c) Release kinetics of protein from nanogel network at different pH determined by HPLC. Reproduced from ref. 45. Copyright 2013 Elsevier Ltd.

353x341mm (150 x 150 DPI)



Cell encapsulation and release: (a) Preparation of dPG-azide precursors and injection of precursors and cells into a microfluidic device. (b) Formation of cell-laden microgels with high viability determined by fluorescent live-dead assays. (c) Degradation of microgels. Degradation of microgel particles (d) at different pH values and fluorescence images of one microgel particle incubated at pH 4.5 (e) at the beginning, (f) half-completed degradation, and (g) fully-completed degradation. Reprinted with permission from ref. 32.

Copyright 2013 WILEY-VCH.
278x110mm (272 x 272 DPI)



Formation of microgels by crosslinking hPG and PEG via Michael addition. Reprinted with permission from ref. 63. Copyright 2012 American Chemical Society.
175x150mm (91 x 91 DPI)

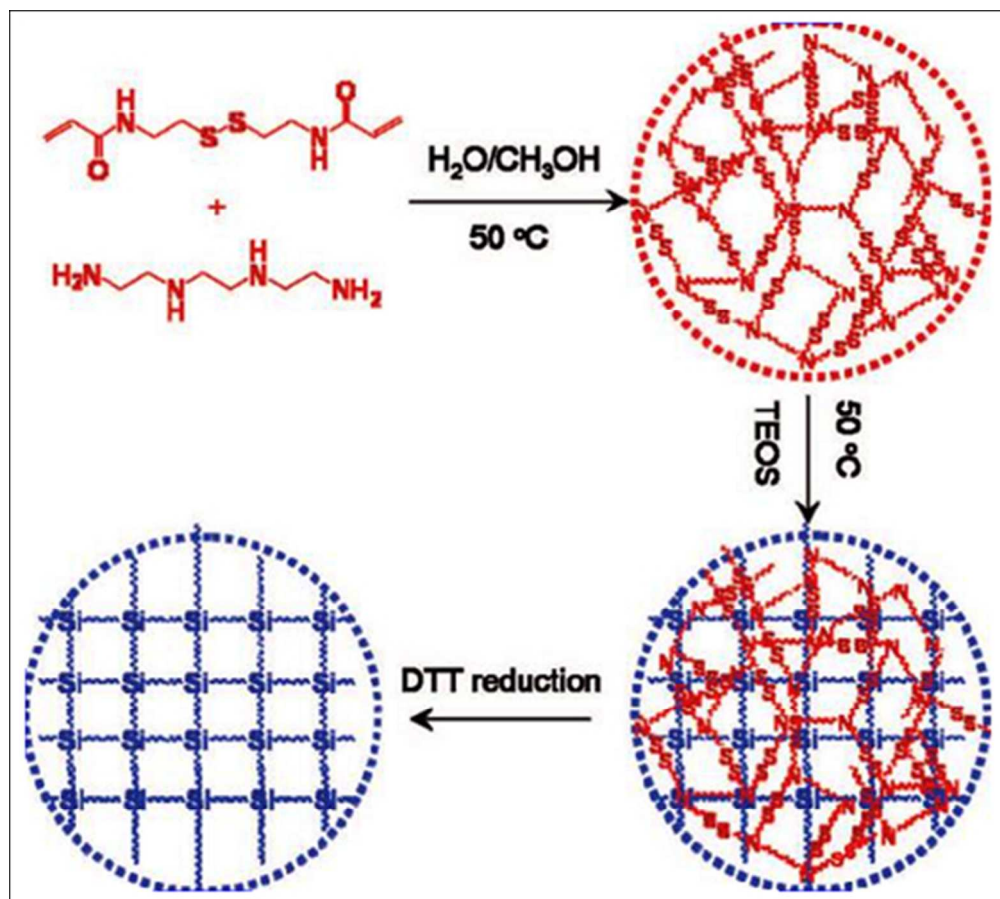
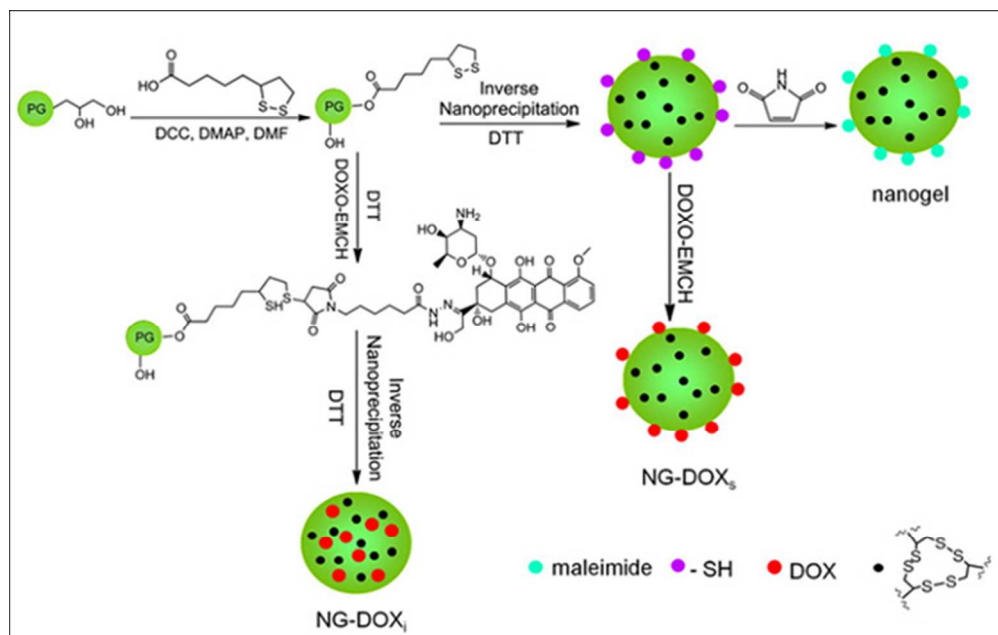
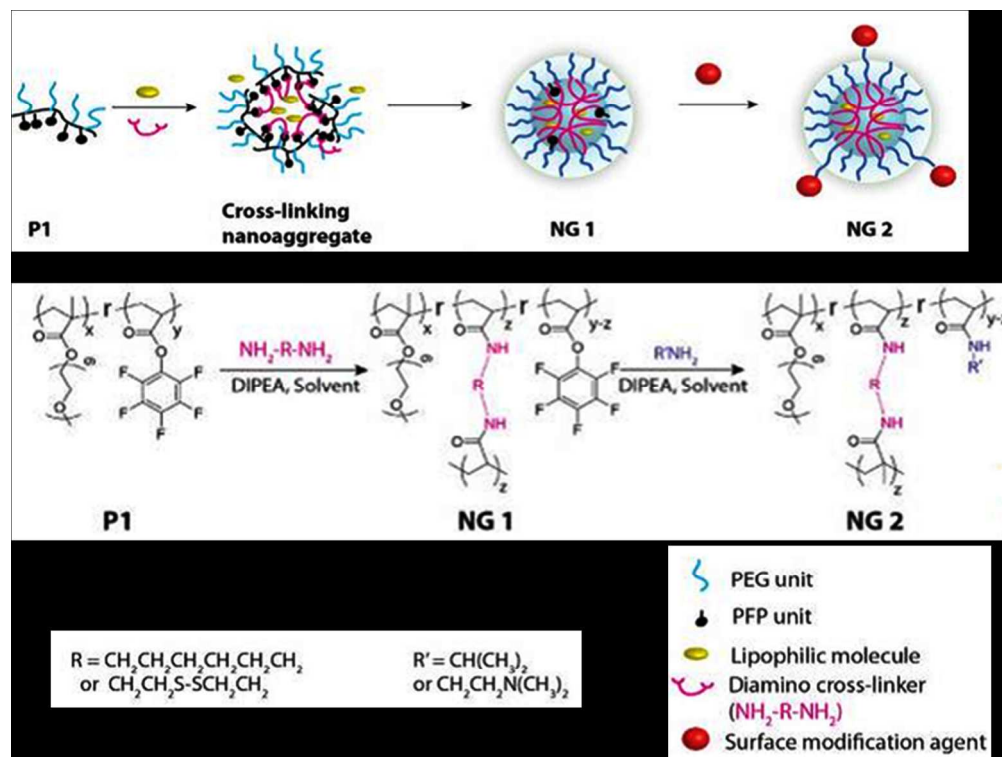


Figure 5. The formation of mesoporous silica spheres from hybrid silica colloids by removal of the nanogels with DTT. Reprinted with permission from ref. 64. Copyright 2009 American Chemical Society. 168x150mm (80 x 80 DPI)

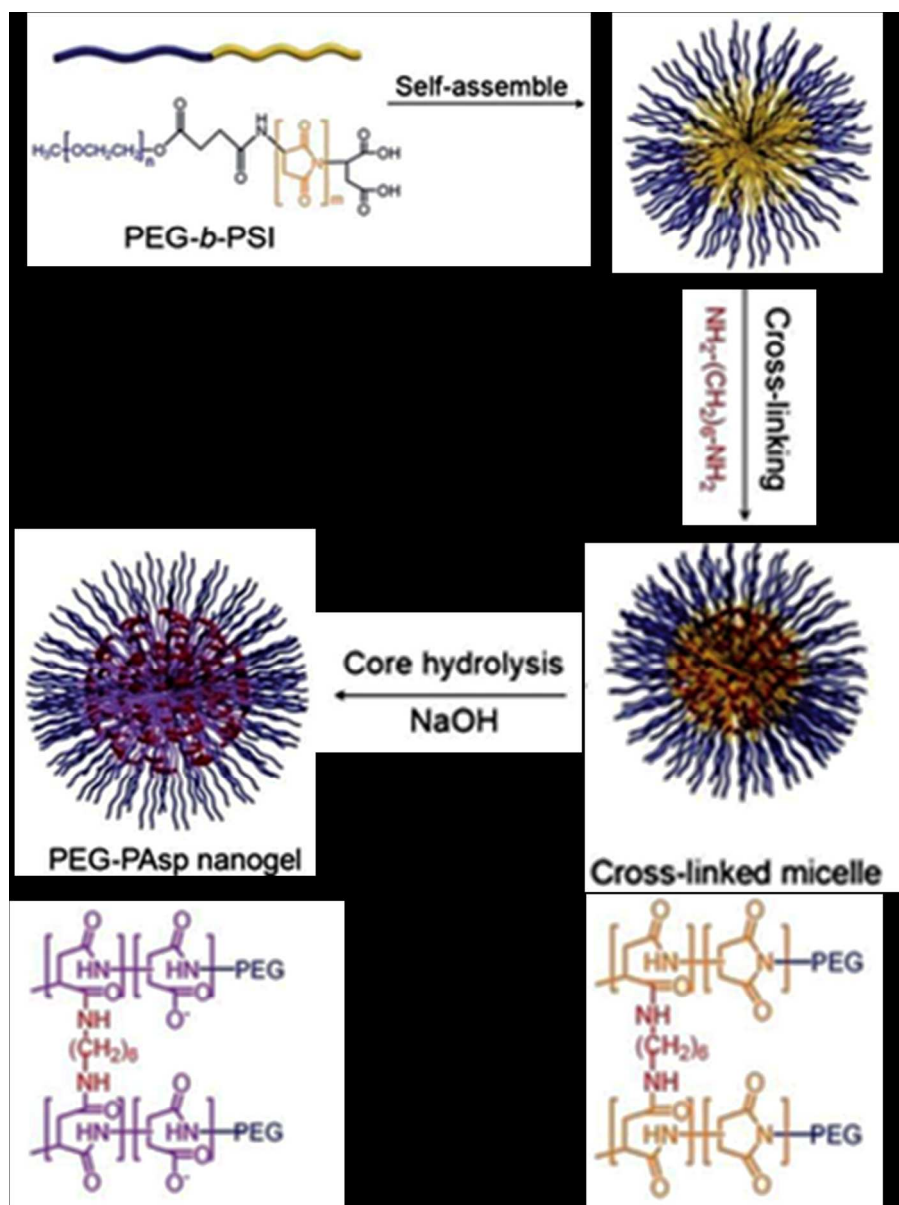


Synthetic approaches of nanogel and prodrug nanogel. Reprinted with permission from ref. 38. Copyright 2014 Elsevier Ltd.

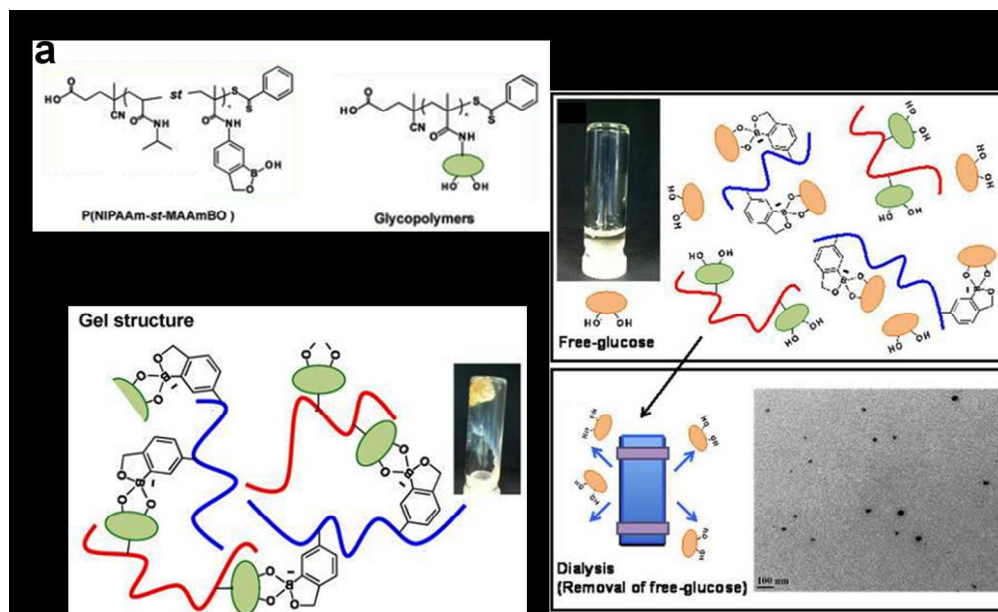
251x165mm (69 x 66 DPI)



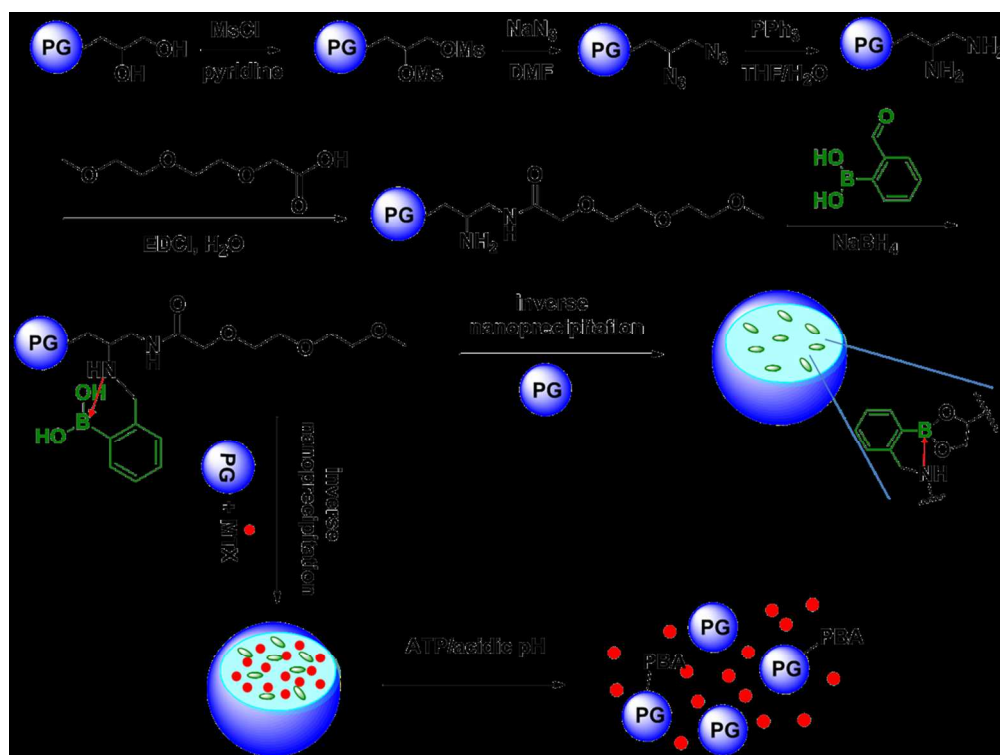
Schematic illustration of synthesis and surface modifications of the crosslinked nanogels. Reprinted with permission from ref. 79. Copyright 2012 American Chemical Society.
254x191mm (150 x 150 DPI)



Synthesis of the PEG-PAsp nanogel. Adapted from ref. 80. Copyright 2013 Royal Society of Chemistry. 206x274mm (150 x 150 DPI)



(a) Formation of gel by boronic-diol interaction between P(NIPAAm-st-MAAmBO) and glycopolymers. (b) Formation of nanogels by adding excess free glucose solution into the gel sample and extensive dialysis in pH 12 solution at 4 °C, and a TEM image of the nanogels. Reprinted with permission from ref. 91. Copyright 2013 American Chemical Society.
307x186mm (150 x 150 DPI)



Synthetic approaches of boronic ester nanogels and Methotrexate (MTX)-loaded nanogels. Reprinted with permission from ref. 92. Copyright 2014 WILEY-VCH. 201x150mm (150 x 150 DPI)

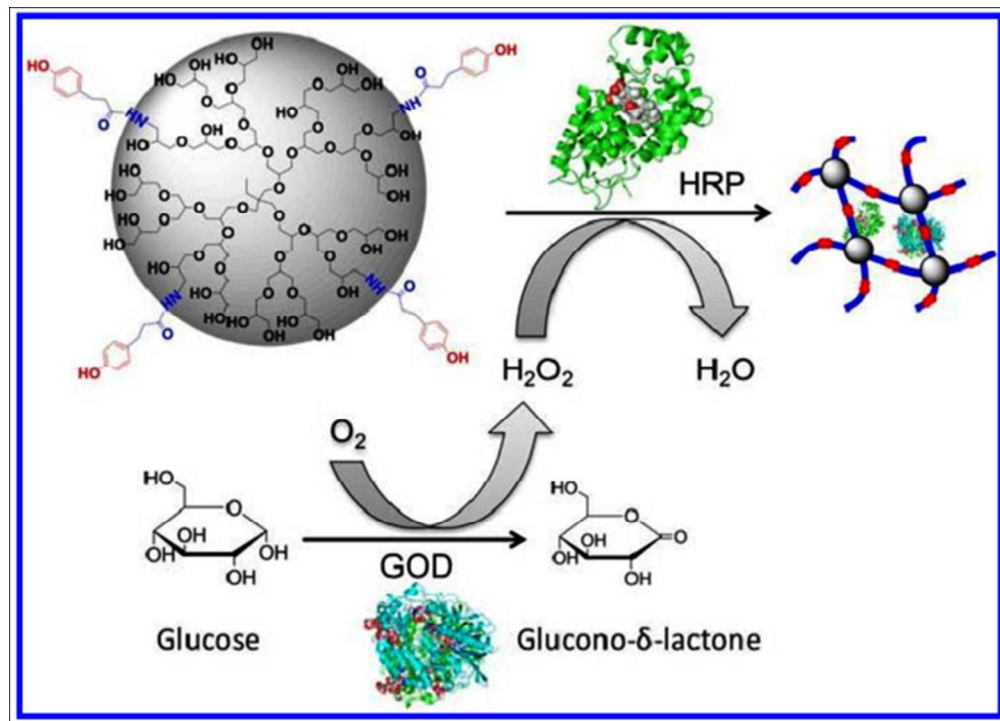
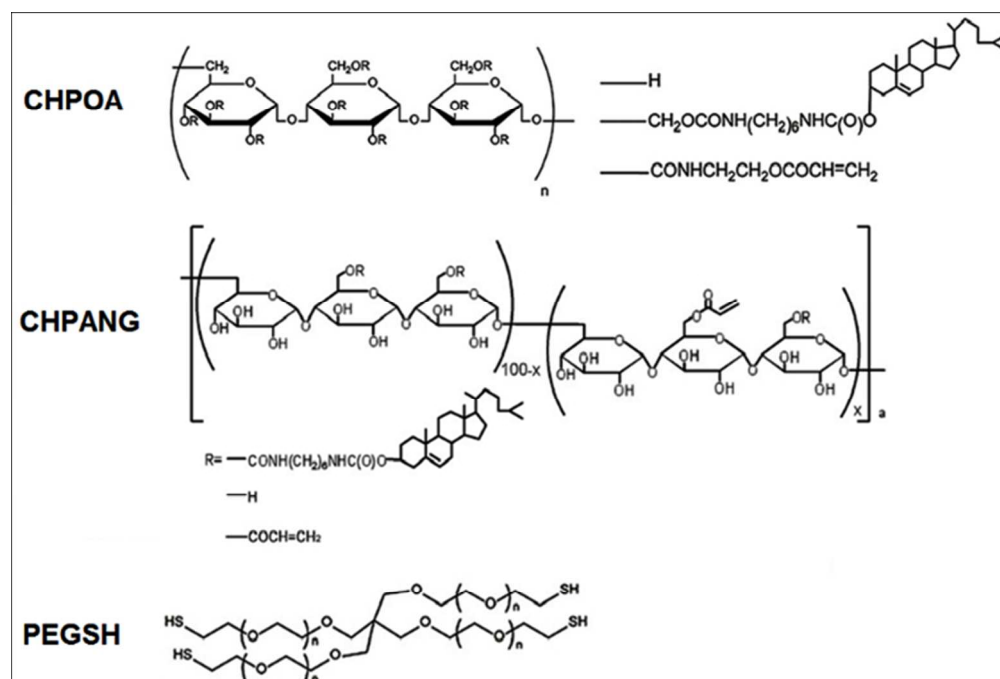
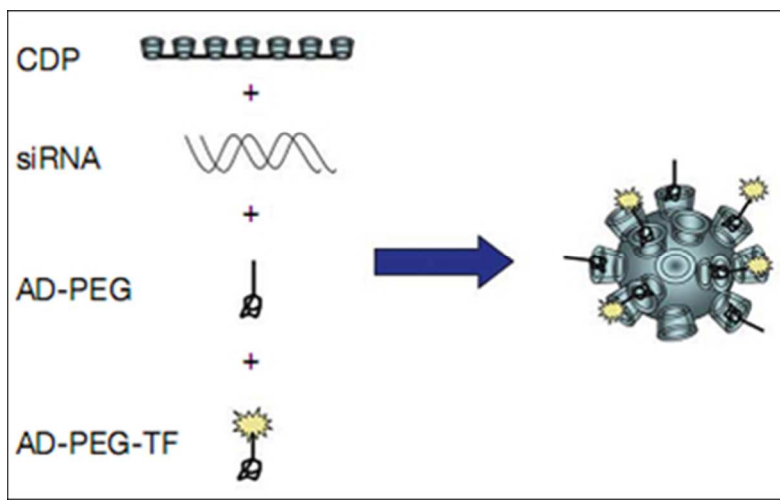


Illustration of hPG-HPA hydrogel formation by HRP crosslinking. Reprinted with permission from ref. 97.
Copyright 2014 American Chemical Society.
209x150mm (87 x 87 DPI)

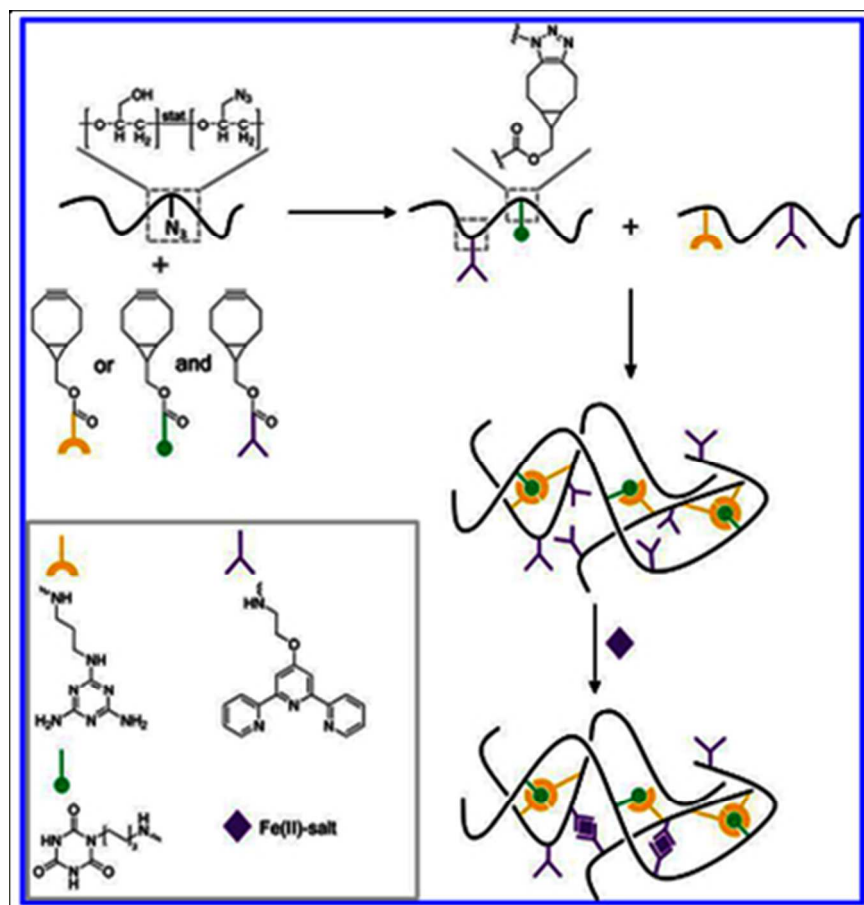


Structures of CHPOA, CHPANG, and PEGSH. Adapted from ref. 31 and 103. Copyright 2012 and 2009 Elsevier.

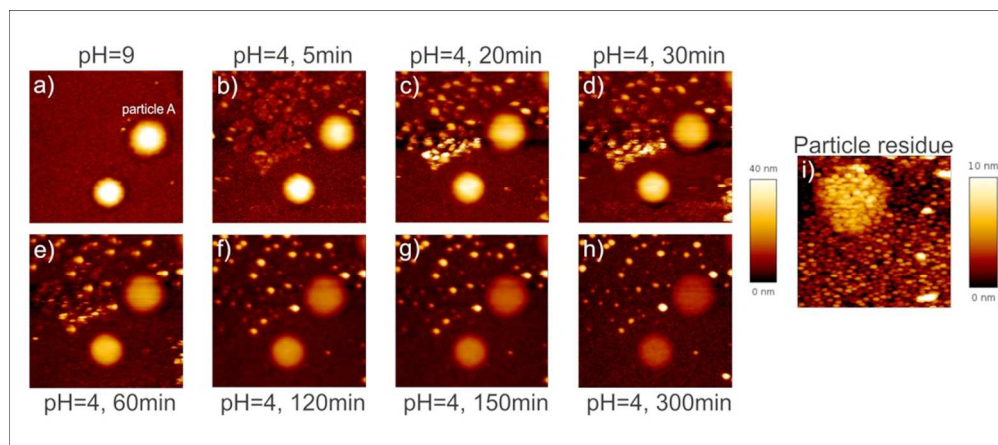
251x169mm (80 x 80 DPI)



Formation of targeted nanoparticles. Reprinted with permission from ref. 113. Copyright 2010 Nature Publishing Group.
243x151mm (41 x 41 DPI)



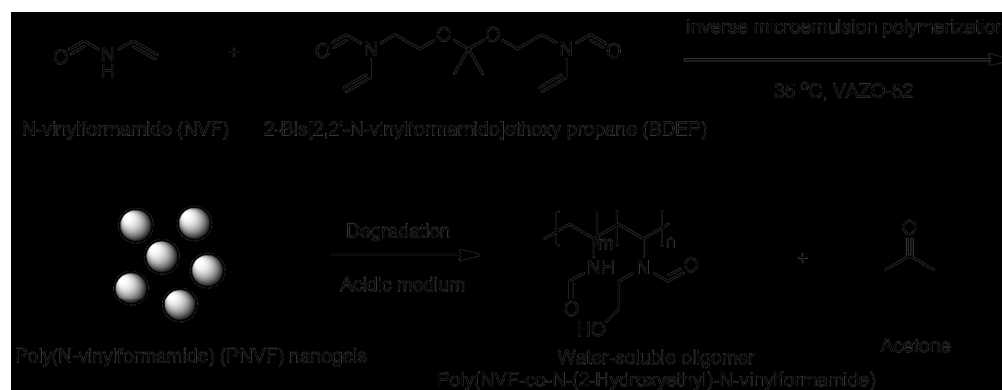
Supramolecular hydrogels formation crosslinked by multiple hydrogen bonding and metal complexation.
Reprinted with permission from ref. 117. Copyright 2014 American Chemical Society.
196x200mm (56 x 57 DPI)



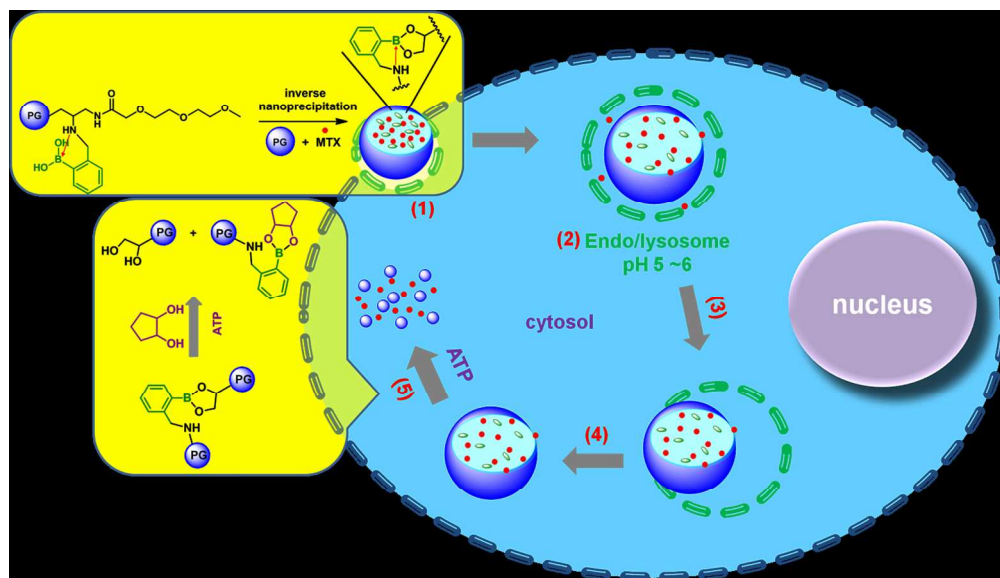
AFM images of the degradation process of polyglycerol nanogels (a-h, scan size: $5 \times 5 \mu\text{m}$) over time in liquid state. Picture I shows the nanogel residue in ambient conditions after degradation (scan size: $2 \times 2 \mu\text{m}$).

Reprinted with permission from ref. 128. Copyright 2014 WILEY-VCH.

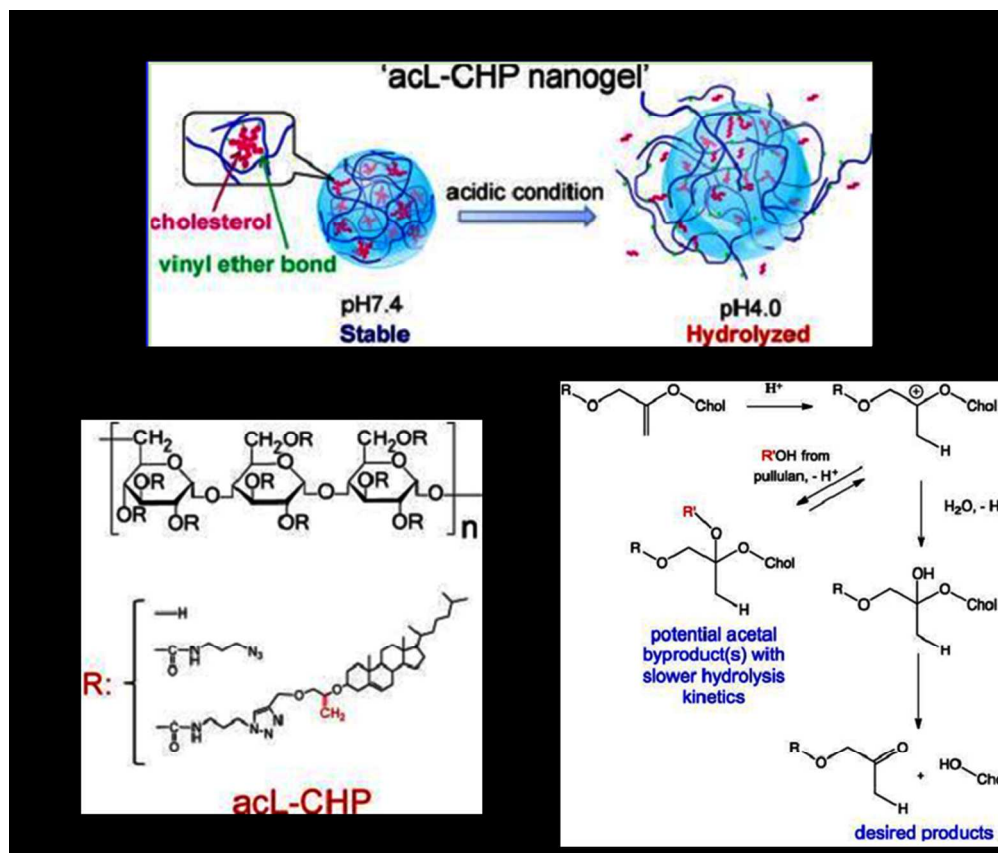
340x150mm (104 x 104 DPI)



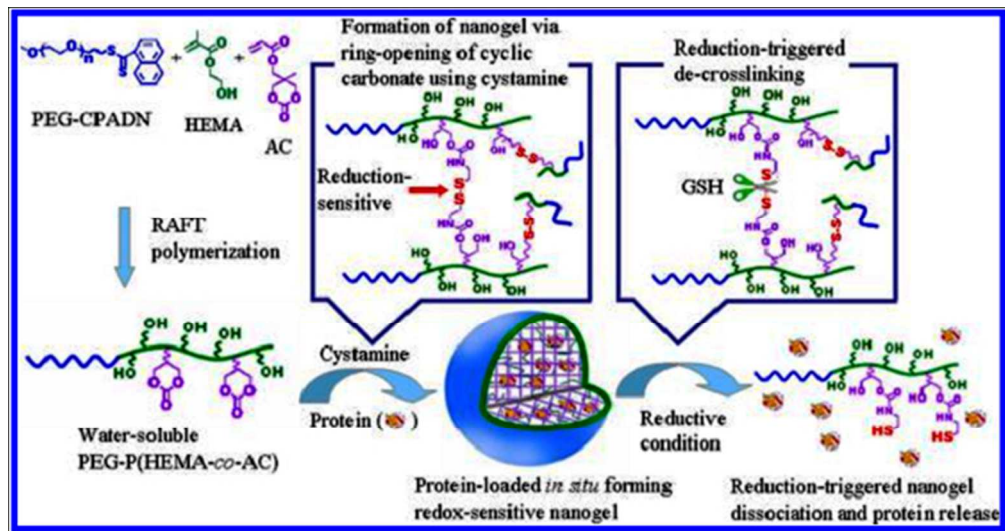
Synthetic approach for acid-labile PNVF nanogels. Reproduced from ref. 129. Copyright 2008 American Chemical Society.
314x120mm (150 x 150 DPI)



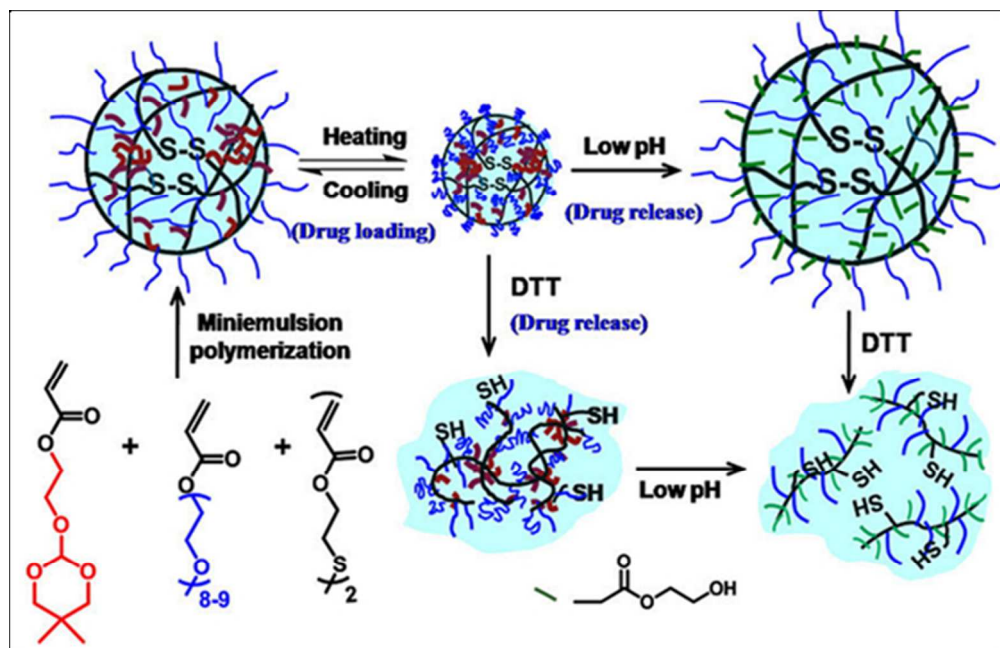
Intracellular pathway of MTX-loaded nanogel: (1) Passive targeting and endocytosis of nanogel, (2) acidity-induced nanogel swelling and protonation of amino groups, (3) disruption of organelle membrane, (4) endo/lysosomal membrane permeation, (5) ATP-triggered dissociation of nanogel. Reprinted with permission from ref. 92. Copyright 2014 WILEY-VCH.
262x150mm (150 x 150 DPI)



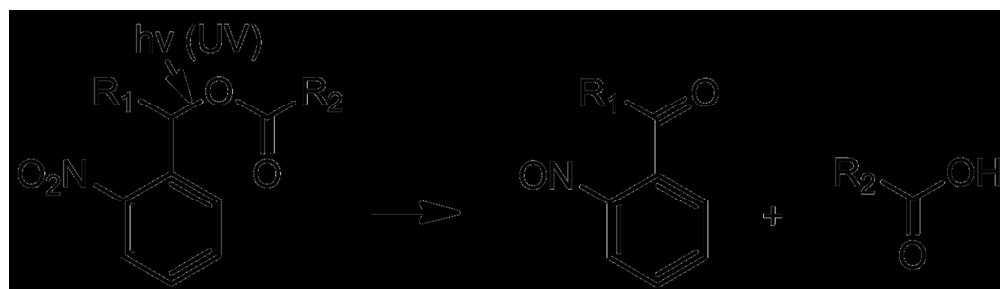
(a) Degradation of acL-CHP nanogel at acidic pH. (b) Chemical structure of acL-CHP. (c) The hypothesis of hydrolysis mechanism of cholesteryl vinyl ether group under acidic conditions. Reprinted with permission ref. 143. Copyright 2013 American Chemical Society.
177x150mm (150 x 150 DPI)



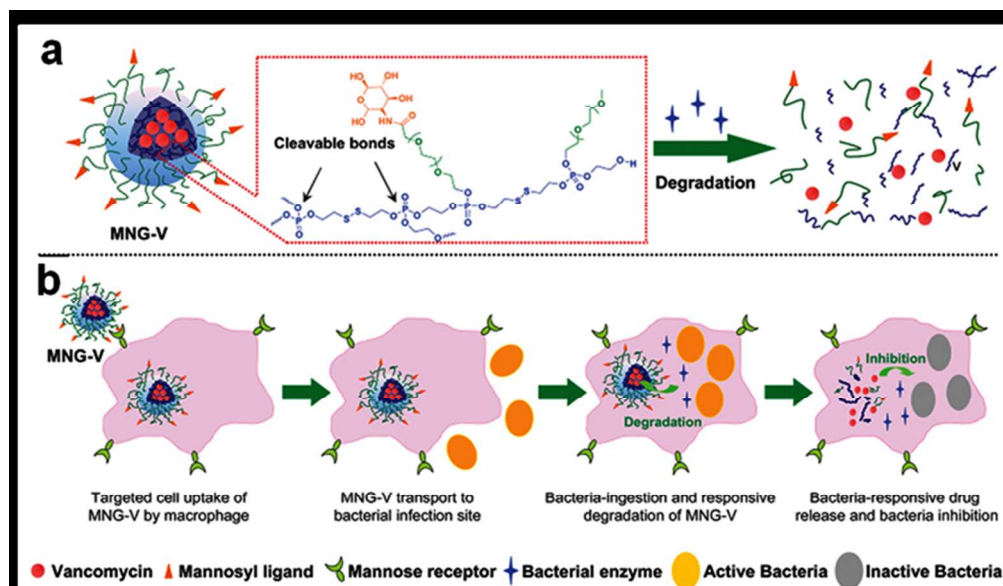
Schematic illustration of the formation of reduction-sensitive nanogels for protein loading and reduction-triggered release. Reprinted with permission from ref. 34. Copyright 2013 American Chemical Society. 292x154mm (61 x 61 DPI)



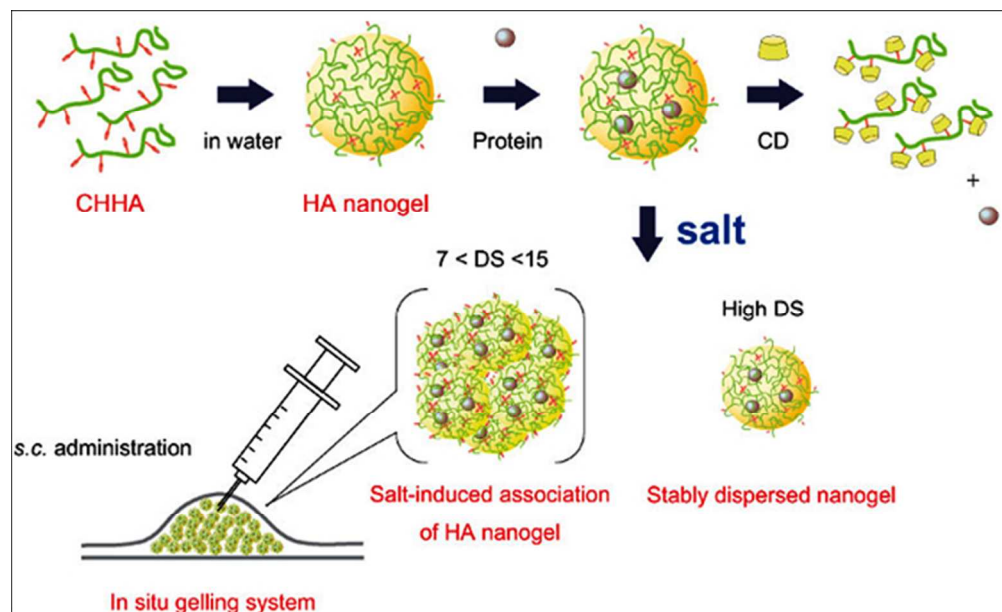
Synthetic pathway and stimuli-responsive behavior of nanogels. Reprinted with permission from ref. 151.
Copyright 2011 WILEY-VCH.
236x150mm (74 x 75 DPI)



Photodegradation of ortho-nitrobenzyl ester derivative.
246x70mm (150 x 150 DPI)



(a) The structure of vancomycin-loaded mannosylated nanogels (MNG-V) and bacteria-responsive drug release, (b) targeted uptake and transport of MNG-V, drug release, and bacteria inhibition. Reprinted with permission from ref. 42. Copyright 2012 WILEY-VCH. 286x177mm (79 x 74 DPI)



The formation of HA nanogel and its solution properties. Reprinted with permission from ref. 102. Copyright 2012 WILEY-VCH.
294x178mm (60 x 60 DPI)